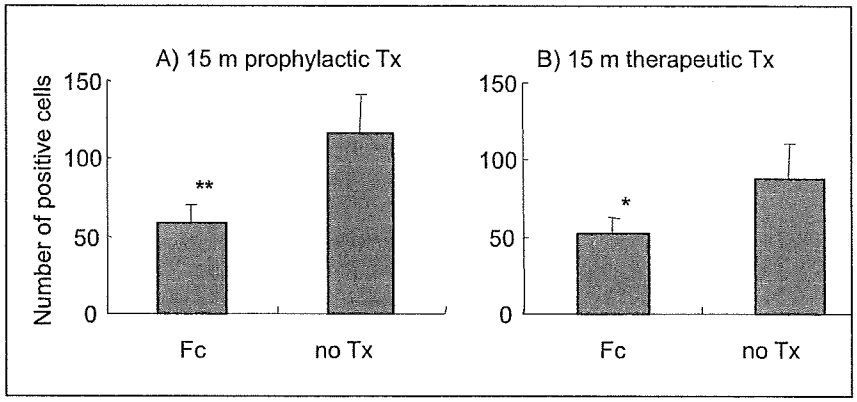

Fig. 7. Quantitative analysis of intracellular Aβ depositions after the prophylactic (A) and therapeutic (B) treatment with Aβ-Fc vaccine at 15 months of age. Microphotographs of the cerebral cortex (8 fields/mouse) were taken and neurons containing Aβ depositions were counted in a blinded manner. The numbers of positive neurons in vaccinated mice were significantly reduced compared with those in untreated mice ($*p < 0.05$; $**p < 0.01$).

and empty vector-vaccinated mice. Double staining with 6F/3D (anti-Aβ) and Iba-1 (antimicroglia) demonstrated the increase of phagocytizing microglia in the cerebral cortex of vaccine-treated Tg mice (unpublished data). It suggests that Aβ phagocytosis by activated microglia is a major pathway of Aβ clearance during nonviral DNA vaccine therapy.

The safety of our vaccines has been established as well as the effects. T-cell activation and proliferation, [^{3}H]-thymidine incorporation of T cells from vaccinated mice was negative in both wild-type B6 and APP23 Tg mice strain. Pathological examinations using monoclonal antibodies, CD5 (anti-T cell) and Mac-3 (anti-macrophage) demonstrated no inflammatory lesion in the brain after long-term treatments (data not shown). Thus, our nonviral Aβ DNA vaccines are highly effective and safe and promising as vaccine therapy against human Alzheimer's disease.

Conclusions

Although interrupted, the phase II clinical trial of AN-1792 provides further support for Aβ immunotherapy of Alzheimer's disease. Alternative vaccine therapies have been investigated and developed to reduce excessive immune reactions of the host brain. As discussed in this article, nonviral DNA vaccines are being introduced as a promising therapy against human Alzheimer's disease.

Acknowledgements

Part of our data and figures are reproduced with copyright permission from *Proceedings of the National Academy of Sciences*.[30]

References

1. Citron, M. *Alzheimer's disease: Treatments in discovery and development.* Nat Neurosci 2002, 5(Suppl): 1055–7.
2. Hardy, J. and Allsop, D. *Amyloid deposition as the central event in the aetiology of Alzheimer's disease.* Trends Pharmacol Sci 1991, 12: 383–8.
3. Schenk, D., Barbour, R., Dunn, W. et al. *Immunization with amyloid-beta attenuates Alzheimer-disease-like pathology in the PDAPP mouse.* Nature 1999, 400: 173–7.
4. Morgan, D., Diamond, D.M., Gottschall, P.E. et al. *A beta peptide vaccination prevents memory loss in an animal model of Alzheimer's disease.* Nature 2000, 408: 982–5.
5. Janus, C., Pearson, J., McLaurin, J. et al. *A beta peptide immunization reduces behavioural impairment and plaques in a model of Alzheimer's disease.* Nature 2000, 408: 979–82.
6. Bard, F., Cannon, C., Barbour, R. et al. *Peripherally administered antibodies against amyloid beta-peptide enter the central nervous system and reduce pathology in a mouse model of Alzheimer disease.* Nat Med 2000, 6: 916–9.
7. DeMattos, R.B., Bales, K.R., Cummins, D.J. et al. *Peripheral anti-A beta antibody alters CNS and plasma A beta clearance and decreases brain A beta burden in a mouse model of Alzheimer's disease.* Proc Natl Acad Sci U S A 2001, 98: 8850–5.
8. Wilcock, D.M., Munireddy, S.K., Rosenthal, A. et al. *Microglial activation facilitates Abeta plaque removal following intracranial anti-Abeta antibody administration.* Neurobiol Dis 2004, 15: 11–20.
9. Bard, F., Barbour, R., Cannon, C. et al. *Epitope and isotype specificities of antibodies to beta-amyloid peptide for protection against Alzheimer's disease-like neuropathology.* Proc Natl Acad Sci U S A 2003, 100: 2023–8.
10. Bacskai, B.J., Kajdasz, S.T., McLellan, M.E. et al. *Non-Fc-mediated mechanisms are involved in clearance of amyloid-beta in vivo by immunotherapy.* J Neurosci 2002, 22: 7873–8.
11. Solomon, B., Koppel, R., Frankel, D. and Hanan-Aharon, E. *Disaggregation of Alzheimer beta-amyloid by site-directed mAb.* Proc Natl Acad Sci U S A 1997, 94: 4109–12.
12. Dodart, J.C., Bales, K.R., Gannon, K.S. et al. *Immunization reverses memory deficits without reducing brain Abeta burden in Alzheimer's disease model.* Nat Neurosci 2002, 5: 452–7.
13. Matsuoka, Y., Saito, M., LaFrancois, J. et al. *Novel therapeutic approach for the treatment of Alzheimer's disease by peripheral administration of agents with an affinity to beta-amyloid.* J Neurosci 2003, 23: 29–33.
14. Orgogozo, J.M., Gilman, S., Dartigues, J.F. et al. *Subacute meningoencephalitis in a subset of patients with AD after Abeta42 immunization.* Neurology 2003, 61: 46–54.
15. Nicoll, J.A., Wilkinson, D., Holmes, C. et al. *Neuropathology of human Alzheimer disease after immunization with amyloid-beta peptide: A case report.* Nat Med 2003, 9: 448–52.
16. Masters, C.L. and Beyreuther, K. *Alzheimer's centennial legacy: Prospects for rational therapeutic intervention targeting the Abeta amyloid pathway.* Brain 2006, 129: 2823–39.
17. Pfeifer, M., Boncristiano, S., Bondolfi, L. et al. *Cerebral hemorrhage after passive anti-Abeta immunotherapy.* Science 2002, 298: 1379.
18. Tang, D.C., DeVit, M. and Johnston, S.A. *Genetic immunization is a simple method for eliciting an immune response.* Nature 1992, 356: 152–4.
19. Barry, M.A., Lai, W.C. and Johnston, S.A. *Protection against mycoplasma infection using expression-library immunization.* Nature 1995, 377: 632–5.
20. Ulmer, J.B., Donnelly, J.J., Parker, S.E. et al. *Heterologous protection against influenza by injection of DNA encoding a viral protein.* Science 1993, 259: 1745–9.
21. Hoffman, S.L., Doolan, D.L., Sedegah, M. et al. *Nucleic acid malaria vaccines. Current status and potential.* Ann NY Acad Sci 1995, 772: 88–94.
22. Zhang, J., Wu, X., Qin, C. et al. *A novel recombinant adeno-associated virus vaccine reduces behavioral impairment and beta-amyloid plaques in a mouse model of*

Alzheimer's disease. Neurobiol Dis 2003, 14: 365–79.
23. Hara, H., Monsonego, A., Yuasa, K. et al. *Development of a safe oral Abeta vaccine using recombinant adeno-associated virus vector for Alzheimer's disease.* J Alzheimers Dis 2004, 6: 483–8.
24. Kim, H.D., Maxwell, J.A., Kong, F.K. et al. *Induction of anti-inflammatory immune response by an adenovirus vector encoding 11 tandem repeats of Abeta1-6: Toward safer and effective vaccines against Alzheimer's disease.* Biochem Biophys Res Commun 2005, 336: 84–92.
25. Urabe, M., Ding, C. and Kotin, R.M. *Insect cells as a factory to produce adeno-associated virus type 2 vectors.* Hum Gene Ther 2002, 13: 1935–43.
26. Nishikawa, M. and Huang, L. *Nonviral vectors in the new millennium: Delivery barriers in gene transfer.* Hum Gene Ther 2001, 12: 861–70.
27. Nishikawa, M. and Hashida, M. *Nonviral approaches satisfying various requirements for effective in vivo gene therapy.* Biol Pharm Bull 2002, 25: 275–83.
28. Ghochikyan, A., Vasilevko, V., Petrushina, I. et al. *Generation and characterization of the humoral immune response to DNA immunization with a chimeric beta-amyloid-interleukin-4 minigene.* Eur J Immunol 2003, 33: 3232–41.
29. Schiltz, J.G., Salzer, U., Mohajeri, M.H. et al. *Antibodies from a DNA peptide vaccination decrease the brain amyloid burden in a mouse model of Alzheimer's disease.* J Mol Med 2004, 82: 706–14.
30. Okura, Y., Miyakoshi, A., Kohyama, K. et al. *Nonviral Abeta DNA vaccine therapy against Alzheimer's disease: Long-term effects and safety.* Proc Natl Acad Sci U S A 2006, 103: 9619–24.
31. Fernandez-Vizarra, P., Fernandez, A.P., Castro-Blanco, S. et al. *Intra- and extracellular Abeta and PHF in clinically evaluated cases of Alzheimer's disease.* Histol Histopathol 2004, 19: 823–44.

Yoshio Okura and Yoh Matsumoto work in the Department of Molecular Neuropathology at the Tokyo Metropolitan Institute for Neuroscience in Japan. *Correspondence: Yoh Matsumoto, Department of Molecular Neuropathology, Tokyo Metropolitan Institute for Neuroscience, Musashidai 2-6, Fuchu, Tokyo 183-8526, Japan. Tel.: +81-423-25-3881, ext. 4719; Fax: +81-423-21-8678; E-mail:matyoh@tmin.ac.jp.*

ELSEVIER

Journal of Neuroimmunology 194 (2008) 34–43

Journal of
Neuroimmunology

www.elsevier.com/locate/jneuroim

Differential effects of decoy chemokine (7ND) gene therapy on acute, biphasic and chronic autoimmune encephalomyelitis: Implication for pathomechanisms of lesion formation

Il-Kwon Park, Keiko Hiraki, Kuniko Kohyama, Yoh Matsumoto *

Department of Molecular Neuropathology, Tokyo Metropolitan Institute for Neuroscience, Tokyo, Japan

Received 14 August 2007; received in revised form 31 October 2007; accepted 16 November 2007

Abstract

Multiple sclerosis (MS) exhibits several clinical subtypes such as the relapsing–remitting (RR) and secondary progressive (SP) forms. In accordance with this, formation of demyelinating plaques in the central nervous system (CNS) occurs by different mechanisms. In the present study, we induced acute, biphasic and chronic (RR or SP) EAE in rats and examined the effects of decoy chemokine (7ND) gene therapy, which inhibits the migration of macrophages, to address the above issue. Interestingly, it was demonstrated that the clinical signs of acute EAE and the first attack of biphasic EAE were minimally affected, whereas chronic EAE and the relapse of biphasic EAE were completely suppressed with 7ND treatment. In the CNS, the number of infiltrating macrophages was reduced in all the stages of the three types of EAE. These findings suggest that in acute EAE and in the first attack of biphasic EAE, where anti-macrophage migration therapy was almost ineffective, pathogenic T cells are mainly involved in lesion formation. In contrast, the relapse of biphasic EAE and chronic EAE macrophages play a major role in the disease process. Thus, the mechanisms of lesion formation are not uniform and immunotherapy should be performed on the basis of information about the pathomechanisms of autoimmune diseases.

Keywords: Acute; Biphasic; Chronic EAE; Macrophage; 7ND; Gene therapy

1. Introduction

The pathogenesis of multiple sclerosis (MS) and its related disorders such as neuromyelitis optica (NMO) is still poorly understood. One of the reasons for this is that there are many variants in terms of the clinical course (Lublin and Reingold, 1996) and pathology (Lucchinetti et al., 2000). Recent progress has shown that the clinical course of MS consists of the early inflammatory phase and late neurodegenerative phase (Sospendra and Martin, 2005). Moreover, even in the early inflammatory phase, the predominant population of infiltrating cells varies considerably (Lucchinetti et al., 2000; van der Goes et al., 2005). Therefore, it is possible that similar neurological deficits are produced by the different mechanisms. The present study aimed to clarify the precise pathomechanisms of lesion formation by treating different types of experimental autoimmune encephalomyelitis (EAE). For this purpose, we performed the treatment experiments with decoy chemokine gene (7ND) to inhibit macrophage infiltration into the central nervous system (CNS). We reasoned that if certain lesions are formed mainly by macrophages, then clinical and pathological conditions would be greatly improved or completely suppressed by anti-macrophage migration therapy. In contrast, the lesions formed mainly by T cells would be minimally affected or unaffected.

7ND was first developed by Zhang et al. as a potent inhibitor of MCP-1/CCL2, as evidenced by the finding that 7ND specifically inhibits MCP-1/CCL2-mediated monocyte chemotaxis (Zhang et al., 1994). On the basis of these data, 7ND has been used for the treatment of various disease models such as vascular diseases

Abbreviations: EAE, experimental autoimmune encephalomyelitis; CNS, central nervous system; MBP, myelin basic protein; MO, monocyte; MOG, myelin oligodendrocyte glycoprotein; MP, macrophage; PI, post-immunization; RR, relapsing–remitting; SC, spinal cord; SP, secondary progressive.

* Corresponding author. Department of Molecular Neuropathology, Tokyo Metropolitan Institute for Neuroscience, Musashidai 2-6 Fuchu, Tokyo 183-8526, Japan. Tel.: +81 423 25 3881x4719; fax: +81 423 21 8678.

E-mail address: matyoh@tmin.ac.jp (Y. Matsumoto).

0165-5728/$ - see front matter © 2007 Elsevier B.V. All rights reserved.
doi:10.1016/j.jneuroim.2007.11.012

(Egashira, 2003; Egashira et al., 2000), arthritis (Gong et al., 1997) and pulmonary hypertension (Ikeda et al., 2002). In all these diseases, macrophages play an essential role in lesion formation and 7ND treatment was found to be effective.

In a previous study, we demonstrated that the neutralization of MCP-1/CCL2 with decoy chemokine receptor gene encoding the binding site of CCR2, which is a receptor for MCP-1/CCL2, significantly suppresses the relapse, but not the first attack, of biphasic EAE (Matsumoto et al., 2005). This suggested that EAE lesions in the spinal cord at the first attack are formed by pathomechanisms different from that during the relapse. In the present study, we examined the effects of 7ND, a potent inhibitor of MCP-1/CCL2, on acute, biphasic and chronic EAE to elucidate the differences in the pathomechanisms among three types of EAE. Consequently, we found that acute EAE and the first attack of biphasic EAE were minimally affected by 7ND treatment, whereas the relapse of biphasic EAE and chronic EAE were completely suppressed in the majority of immunized rats by the same treatment. These findings suggest that T cells play a major role in formation of the former lesions and that macrophages are essential effectors for the latter lesion formation. Thus, immunotherapy should be performed on the basis of information about the pathomechanisms of lesion formation of autoimmune diseases.

2. Materials and methods

2.1. Animals

LEW.1AV1 rats were kindly provided by Dr. R. Gold, Department of Neurology, Wuerzburg University, Germany and maintained in our animal facility. Lewis (LEW) and DA rats were purchased from Japan SLC Inc. (Shizuoka). All rats used were 8–12 weeks of age.

2.2. Reagents

Recombinant rat MOG was prepared as described previously (Sakuma et al., 2004). Briefly, the gene coding the extracellular domain (amino acid 1–125) of MOG was amplified using primers specific for the corresponding MOG sequence. The PCR products were then digested with Sph I and Hind III and subcloned into pQE30 (QIAGEN, Tokyo, Japan) for large-scale preparation. Recombinant MOG in transformed *E. coli* was isolated under denaturing conditions and purified using Ni-NTA Agarose (QIAGEN). Then, purified MOG was diluted and refolded in PBS containing 1 M L-arginine, 2 mM glutathione (reduced form) and 0.2 mM glutathione (oxidized form). The obtained protein contained endotoxins less than 10 EU/1 mg protein as determined with a Toxinometer ET-2000 (Wako, Tokyo, Japan).

The myelin fraction was extracted from bovine spinal cords as described previously with a few modifications (Agrawal et al., 1972; Casado et al., 1988). Briefly, spinal cord tissue was homogenized and washed in 0.32 M sucrose and the suspension was overlaid on 0.84 M sucrose. After centrifugation, the interface was collected, washed with Milli Q water and homogenized. Using fractions other than the interface, this process was repeated and the interface was collected. These preparations were lyophilized and kept at −80 °C until use. Western blot analysis revealed that the purified myelin preparation contained myelin basic protein (MBP), proteolipid protein (PLP) and MOG (data not shown). Guinea pig, bovine and rat MBP were prepared as described previously (Deibler et al., 1972).

2.3. Preparation of 7ND plasmid and gene therapy

Total RNA was isolated from the spleen of a normal Lewis rat using RNAzol ™ B (TEL-TEST INC.). The RNA was subjected to reverse transcription using ReverTra Ace-α- ™ (TOYOBO, Osaka, Japan) and amplification with specific primers (sense, GACTCGAGACCATGCAGGTCACCTGCTGCTAT; anti-sense, GAGCGGCCGCTCAAGTCTTCGGAGTTTGGG) was performed as shown in previous studies (Egashira et al., 2000; Zhang et al., 1994). The PCR fragment was then cloned into the pCR^{R}4Blunt-TOPO cloning vector (Invitrogen, Tokyo, Japan) and sequenced to confirm that the plasmid contains the insert with the right sequence. The resulting pCR^{R}4Blunt-TOPO 7ND was subjected to enzymatic digestion with Xho I-Not I (210 bp) and ligated into the Xho I-Not I site of pTARGET (Promega, Tokyo, Japan), which was used for the experiments.

7ND at a dose of 100 μg was administered intramuscularly three times a week between days 0 and 21 post-immunization. Control rats were given an empty vector at the same dose with the same protocol.

2.4. EAE induction and clinical evaluation

Three types of EAE, acute, biphasic and chronic EAE were induced by the following methods. Acute EAE was induced in LEW rats by immunization with MBP and biphasic EAE was induced in DA rats by immunization with myelin (Matsumoto et al., 2005). In both cases, the onset of the disease and maximal severities were relatively uniform. Chronic EAE was induced in LEW.1AV1 rats by immunization with recombinant MOG. The clinical course of the disease was variable and the majority of rats showed the relapsing–remitting (RR) or the secondary progressive (SP) form as described previously (Sakuma et al., 2004). Clinical signs were evaluated as the total score of the degree of paresis of each limb and tail (partial paresis, 0.5; complete paresis, 1.0). Therefore, the clinical score of complete paralysis of four limbs plus tail or the moribund conditions was 5.

2.5. Histological and immunohistochemical examinations

The optic nerve, cerebrum, brain stem, cerebellum and the cervical, thoracic and lumbar spinal cord were routinely examined. The tissues were fixed in 4% paraformaldehyde and processed for paraffin embedding. Six μm sections were cut and stained with hematoxylin and eosin (H&E) and with Kruever and Barrera's (K–B) method. Inflammatory lesions were graded using sections stained with H&E and W3/13 for T cells into four categories (Grade 1, leptomeningeal and adjacent subpial cell

infiltration; Grade 2, mild perivascular cuffing; Grade 3, extensive perivascular cuffing; Grade 4, extensive perivascular cuffing and severe parenchymal cell infiltration). Demyelinating lesions were graded using sections stained with the K–B method into five categories (Grade 1, trace of perivascular or subpial demyelination; Grade 2, focal demyelination; Grade 3, demyelination involving a quarter of tissues examined; Grade 4 massive confluent demyelination involving half of the tissue; Grade 5, extensive demyelination involving the entire tissues. Macrophage infiltration was evaluated by counting ED1-positive cells under high magnification and expressed as % ED1-positive cells (ED1-positive cells/ED1-positive plus ED1-negative cells × 100).

Single immunoperoxidase staining was performed as desribed previously (Matsumoto and Fujiwara, 1987; Ohmori et al., 1992). Briefly, paraffin-embedded sections were deparaffinized and rehydrated. After blocking the endogenous peroxidase activity with methanol containing 0.3% hydrogen peroxide, the sections were incubated with mAb W3/13 (Dainippon Pharm, Osaka, Japan) for T cell-staining or ED1 (purified from the hybridoma supernatant) for macrophage-staining. After washing, the sections were incubated with

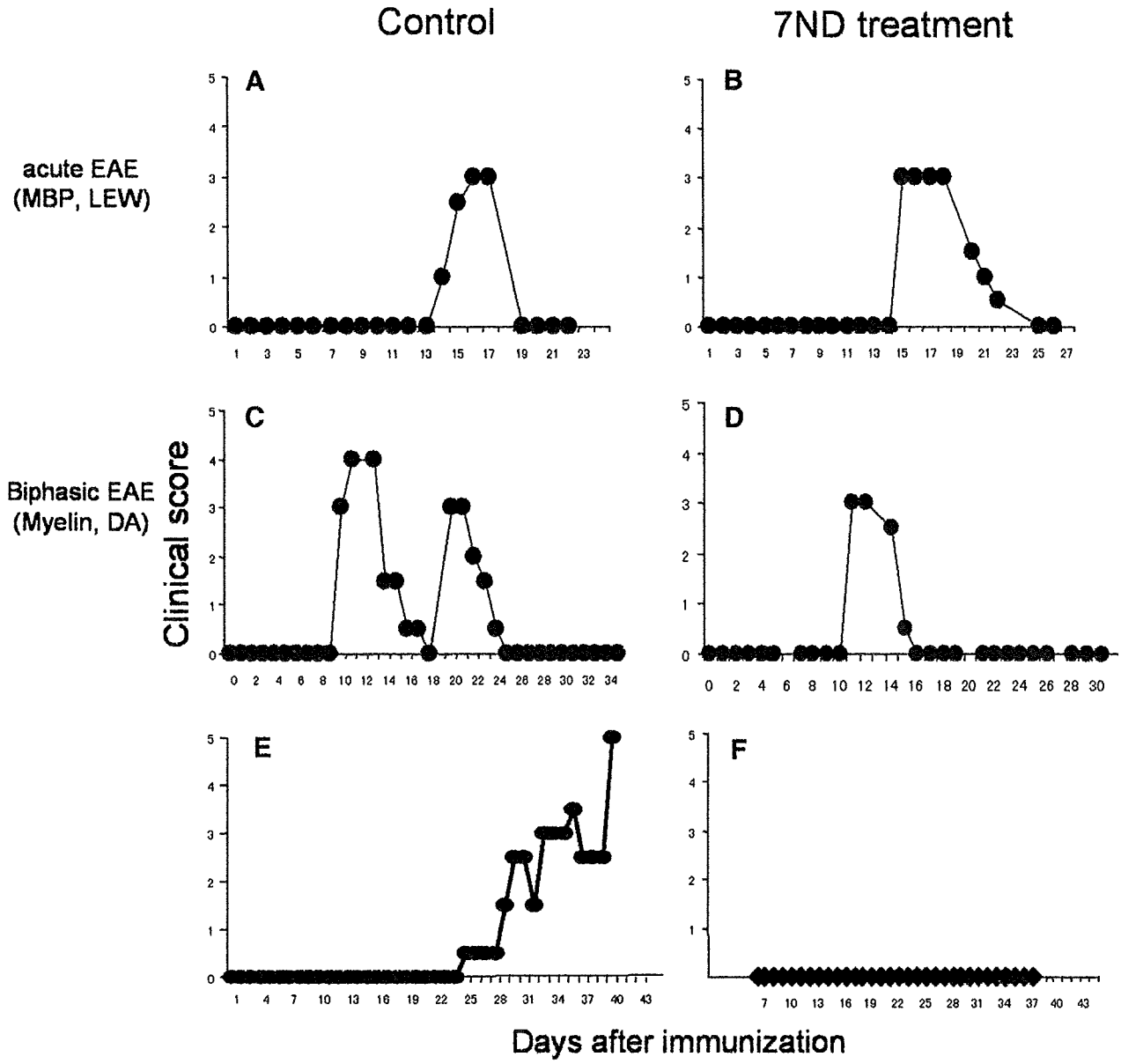

Fig. 1. Modulation of the clinical course of acute, biphasic and chronic EAE by 7ND treatment. In acute EAE, there is no significant change in the clinical course between control (A) and 7ND-treated (B) rats. Treatment with 7ND of rats immunized with myelin results in complete suppression of the relapse (D) found in control rats (C), while the first attack is suppressed slightly. In chromic EAE, treated rats (F) did not develop EAE at all, while the control rats had severe and continuous clinical signs (E). The representative clinical courses of individual rats with acute, biphasic and chronic EAE are illustrated. Acute and biphasic EAE showed relatively uniform clinical courses and did not show any further relapse by day 60 (unpublished observations). In contrast, LEW.1AV1 rats immunized with MOG developed the relapsing–remitting or secondary progressive form of chronic EAE. In (E), secondary progressive EAE is shown.

biotinylated anti-mouse IgG (Vector, Burlingame, CA) followed by horseradish peroxidase (HRP)-labeled VECTSTAIN Elite ABC Kit (Vector). HRP-binding sites were detected in 0.005% diaminobenzidine and 0.01% hydrogen peroxide. To confirm the specificity of the staining, the primary antibodies were omitted or replaced with normal mouse IgG. The controls did not show any specific staining.

2.6. ELISA

The levels of anti-MOG and anti-MBP antibodies were measured using ELISA. Recombinant MOG or purified MBP (10 μg/ml) were coated onto microtiter plates and serially diluted sera from normal and immunized animals were applied. After washing, appropriately diluted horseradish-conjugated anti-rat IgG was applied. The reaction products were then visualized after incubation with the substrate. The absorbance was read at 450 nm.

2.7. Real-time PCR

After residual genomic DNA was removed with DNase (TURBO DNA-free ™, Ambion, Tokyo, Japan), first strand cDNA was synthesized from 1 μg of total RNA using random hexamers and ReverTra Ace (TOYOBO). SYBR Green real-time PCR reactions were performed on an ABI PRISM 7500 sequence detection system (Applied Biosystems, Foster City, CA) in a total volume of 25 μl using the SYBR Premix Ex Taq (Takara Bio, Otsu, Japan). Each PCR was performed in duplicate under the following thermocycler conditions: stage 1, 95 °C for 10 min for one cycle and stage 2, 95 °C for 15 s and 58 °C for 1 min for 50 cycles. All primers, except for 18 S rRNA, were designed on an intron–exon junction to prevent the coamplification of genomic DNA. The relative quantification of mRNA was performed using the standard curve method. Cytokine mRNA was normalized to 18 S RNA for each sample (Bas et al., 2004). The absence of nonspecific amplification was confirmed by the dissociation curve analysis.

2.8. Statistical analysis

Data were analyzed by Student's *t* test or Mann–Whitney's *U*-test. *P*-value less than 0.05 was considered as statistically significant.

3. Results

3.1. Clinical course and pathology of acute, biphasic and chronic EAE

In the present study, we induced acute, biphasic and chronic EAE by the immunization protocols as reported in detail previously (Kim et al., 1998; Matsumoto et al., 2005; Sakuma et al., 2004). The representative clinical courses of individual rats with acute, biphasic and chronic EAE are illustrated in Fig. 1A, C and E, respectively, and all the results are summarized in Table 1. Acute EAE was induced in LEW rats by immunization with MBP. As shown in Fig. 1A and Table 1 (Group B), rats developed acute monophasic EAE with the onset of day 12.3±0.5 and the maximal clinical score was 2.9±0.2. Immunization of DA rats with purified myelin-induced biphasic EAE with the fist peak on day 9.3±0.8 with the maximal clinical core of 4, followed by the relapse on day 17.8±0.8 with the clinical score of 3.0±0.4 (Fig. 1C and Table 1, Group D). These two types of EAE showed relatively uniform clinical courses and did not show any further relapse by day 60 (unpublished observations). In contrast, LEW.1AV1 rats immunized with MOG developed RR or SP form of chronic EAE as shown in a previous study (Sakuma et al., 2004). In Fig. 1E, SP EAE is shown.

3.2. 7ND treatment modulates biphasic and chronic, but not acute, EAE

7ND (100 μg), a dominant inhibitor of MCP-1/CCL2 (Zhang et al., 1994), was injected intramuscularly three times a week from day 0 to day 21 to rats that had been immunized for acute, biphasic and chronic EAE. Control rats received an empty vector. The representative clinical courses of treated animals are shown in Fig. 1B, D and F and all the data are summarized in Table 1. Interestingly, 7ND modulated the clinical course of three types of EAE very differently. Acute EAE was influenced very slightly by 7ND treatment (Fig. 1A and B). All the treated rats developed severe EAE with a maximal clinical score of 2.4±0.7 (Table 1, Group A) and there was no significant difference between the treated and control groups. In contrast, biphasic EAE was modulated characteristically. As depicted in Fig. 1C and D and summarized in Table 1, Groups C and D, the clinical score during the first attack was slightly suppressed compared with that of the control rats but all the rats developed severe EAE. Interestingly,

Table 1
Summary of clinical courses of acute, biphasic and chronic EAE of rats treated with 7ND

Group	Ag	Strain	Treatment		Incidence	Onset	Max. clininical sign
A	MBP	LEW	7ND		7/7	13.3±0.9	2.4±0.7
B			Control		3/3	12.3±0.5	2.9±0.2
C	Myelin	DA	7ND	1st attack	4/4	10.8±0.4	3.0±0.7
				Relapse	0/4	(−)	(−)
D			Control	1st attack	4/4	9.3±0.8	4
				Relapse	4/4	17.8±0.8	3.0±0.4
E	MOG	LEW.1AV1	7ND		1/5	36	2.5
F			Control		5/5	27.8±3.7	3.9±0.9

LEW, DA and LEW.1AV1 rats were immunized with MBP, myelin and MOG, respectively, and observed daily for clinical signs. Observation periods were 21–23 days for acute EAE, 31–34 days for biphasic EAE and 37–40 days for chronic EAE. Rats listed in Tables 2 and 3 are not included in this table.

the relapse of the disease was completely suppressed by the treatment (Table 1, Group C vs. D). Finally, chronic EAE induced by immunization with MOG was completely suppressed in 4 out of 5 rats by the treatment (Fig. 1F and Table 1, Group E).

3.3. Pathological changes in treated animals

As biphasic and chronic, but not acute, EAE was affected by 7ND treatment, we tried to characterize pathology of biphasic and chronic EAE in treated animals and compared the results with those obtained from control rats. At the first attack of biphasic EAE, there was marked macrophage infiltration in control rats (Fig. 2A). In 7ND-treated rats at the same period, the number of infiltrating macrophages was reduced but some were present in the lesion (indicated by arrow heads in Fig. 2B). During the relapse of biphasic EAE, many macrophages were detected in the control rats and some of them showed the feature of "foamy macrophages" (arrows in Fig. 2C). 7ND treatment

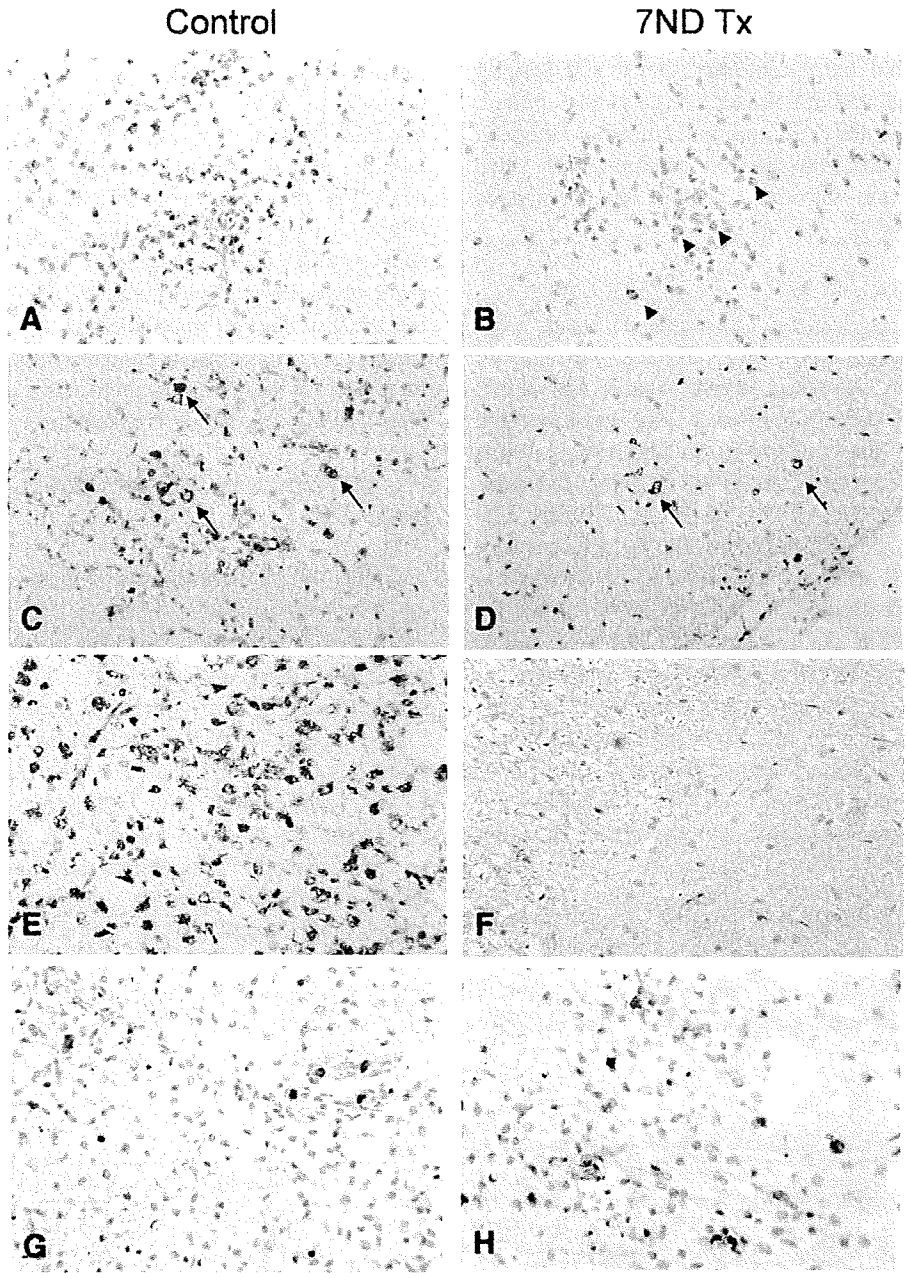

Fig. 2. Immunohistochemical staining of macrophages (A–F) and T cells (G, H) in the spinal cords of the control (A, C, E and G) and 7ND-treated (B, D, F and H) rats. At the first attack of biphasic EAE, there is marked macrophage infiltration in control rats (A). In treated rats with clinical signs at the first attack, the number of infiltrating macrophages is reduced but some are present in the lesion (arrow heads in B). During the relapse of biphasic EAE, many macrophages are detectable in control rats and some of them show the feature of "foamy macrophages" (arrows in C). 7ND treatment reduced the number of inflammatory lesions with macrophages during the same period (arrows in D). In chronic EAE, dense macrophage infiltration found in control rats (E) is completely absent in treated rats (F). In T cell staining, the distribution and density of T cells were not significantly different between the control (G) and treated (H) groups in biphasic EAE (the first attack, histological grade 3). A–F, ED1 staining; G & H, W3/13 staining, ×120.

greatly reduced the number of inflammatory lesions during this period (Fig. 2D). Table 2 summarizes the histological severities of all the treated and control rats with biphasic EAE. At the first attack, the mean histological scores of the spinal cord of treated and control rats were 1.6±1.0 and 2.7±0.8, respectively, and treated rats showed a significantly milder pathology ($p=0.015$). In addition, in treated rats, severe lesions were limited to one or two segments of the spinal cord, while almost the entire spinal cord was involved in control rats (1° in Table 2). During the relapse, treated rats except one case showed no or minimal pathology compared with control rats (2° in Table 2). Infiltration in biphasic EAE was further evaluated by counting ED1-positive cells under high magnification and expressed as % ED1-positive cells (ED1-positive cells/ED1-positive plus ED1-negative cells × 100). The results are shown in Table 3. In control rats, macrophages accounted for 50.2±5.0% during the first attack. During the relapse, the percentage increased slightly but significantly ($p=0.013$). In 7ND-treated rats, macrophage infiltration was significantly inhibited during the first attack and relapse ($p=0.36$ and $p=0.00001$, respectively). The inhibition was more marked during the relapse than during the first attack. These findings were correlated well with the clinical course.

In chronic EAE, dense macrophage infiltration found in control rats (Fig. 2E) was completely absent in treated rats (Fig. 2F). Two of three treated rats were completely normal histologically and one rat without clinical signs showed moderate pathology (Table 4). In contrast, control rats showed moderate to severe inflammation and/or demyelination at least in one segment of the spinal cord (Table 4).

We also examined the distribution and density of infiltrating T cells in the spinal cord of treated and control rats during the first attack of biphasic EAE and found that there was no significant difference between the two groups (Fig. 2G and H). Using spinal cord sections with inflammatory scores of 2–3, we counted W3/13-positive cells/inflammatory lesion in 7ND-treated and control rats and found that there was no significant difference (9.5±3.1 vs. 9.2±3.2, $p=0.87$). These findings suggest that 7ND treatment minimally interfere with T cell infiltration into the CNS lesions. B cell infiltration was not detected throughout the course of chronic EAE (data not shown).

Table 2
Pathology of the CNS of DA rats with myelin-induced EAE after 7ND treatment

	Tx	Sampling	Clinical score[a]	Opt[b]	Cbr	BS/Cbll	C	Th	L
1°	7ND	d12	4	0	0	0	3	2	1
	7ND	d12	3.5	0	0	2	0	3	2
	7ND	d12	3	0	0	1	1	1	1
	7ND	d11	4	0	0	2.5	3.5	2	0
	Control	d11	4	1	0	2	3	3.5	3
	Control	d11	4	0	0	2	2.5	3.5	1
	Control	d12	3	0	0	1	2	3	3
2°	7ND	d19	0 (3)[a]	n.e.[c]	0	0	0	0	0
	7ND	d19	0 (3.5)	1	0	1	0	0	1
	7ND	d19	3 (4)	0	0	0	3	3	0
	7ND	d19	0 (3.5)	0	0	0	1	0	0
	Control	d20	3 (3)	0	n.e.	n.e.	3	3.5	3
	Control	d20	3 (4)	0	n.e.	n.e.	2.5	3.5	1
	Control	d22	2.5 (4.5)	0	0	1/3.5[d]	0	2	0.5
	Control	d22	2 (4)	0	0	1.5	3	2.5	2

Rats listed in Table 1 are not included in this table.
[a] Clinical score at time of sampling. The number in the parenthesis indicates the maximal clinical score throughout the observation periods.
[b] Opt, optic nerve; Cbr, cerebrum; BS/Cbll, brain stem/cerebellum; C, cervical spinal cord; Th, thoracic spinal cord; L, lumbar spinal cord.
[c] n.e.: not examined.
[d] 1/3.5 indicates inflammation score/demyelination score. All other scores indicate inflammation score.

Table 3
The density of infiltrating macrophages in the spinal cord of 7ND-treated and control rats with biphasic EAE

	1st attack	Relapse
7ND	30.2±14.6[a]	12.3±7.4[a]
Control	50.2±5.0[a]	61.9±5.6[a]

Macrophage infiltration was evaluated by counting ED1-positive cells under high magnification ($n=6$ per group) and expressed as % ED1-positive cells (ED1-positive cells/ED1-positive and negative cells × 100). The mean %±SD are shown.
[a] Significant differences were noted in all the following combinations. 7ND 1st attack vs. 7ND Relapse ($p=0.036$); 7ND 1st attack vs. Control 1st attack ($p=0.017$); 7ND Relapse vs. Control Relapse ($p=0.00001$); Control 1st attack vs. Control Relapse ($p=0.013$).

3.4. Chemokine profiles in 7ND-treateed animals

We performed the quantitative analysis of chemokines in the spinal cord of treated and control rats with biphasic EAE (Fig. 3A and C) or with chronic EAE (Fig. 3B and D) using real-time PCR. In control rats with biphasic EAE, MCP-1/CCL2 was mainly upregulated during the first attack (Day 14 in Fig. 3A), whereas MIP-1α/CCL3 increased during both the first attack and relapse (Days 12 and 19 in Fig. 3C). MCP-1/CCL2 and MIP-1α/CCL3 in the spinal cords of treated rats were suppressed slightly during the first attack and almost completely during the relapse. This finding correlated well with the degree of macrophage infiltration (Table 3).

Table 4
Pathology of the CNS of LEW.1AV1 rats with MOG-induced EAE after 7ND treatment

Tx	Sampling	Clinical score[a]	Opt[b]	Cbr	BS/Cbll	C	Th	L
7ND	d43	0	0	0	0	0	0	0
7ND	d43	0	0	0	0	0	0	0
7ND	d43	0	0	2	2/3[c]	0	0	0/3
Control	d35	0.5 (0.5)	0	1	2	0	0	0
Control	d35	3 (3)	1/4	0	0	0	3/4[c]	3/3[c]
Control	d35	1.5 (2.5)	0	1	1	0	0	1/3

Rats listed in Table 1 are not included in this table.
[a] Clinical score at time of sampling. The number in the parenthesis indicates the maximal clinical score throughout the observation periods.
[b] Opt, optic nerve; Cbr, cerebrum; BS/Cbll, brain stem/cerebellum; C, cervical spinal cord; Th, thoracic spinal cord; L, lumbar spinal cord.
[c] 2/3 indicates inflammation score/demyelination score. All other scores indicate inflammation score.

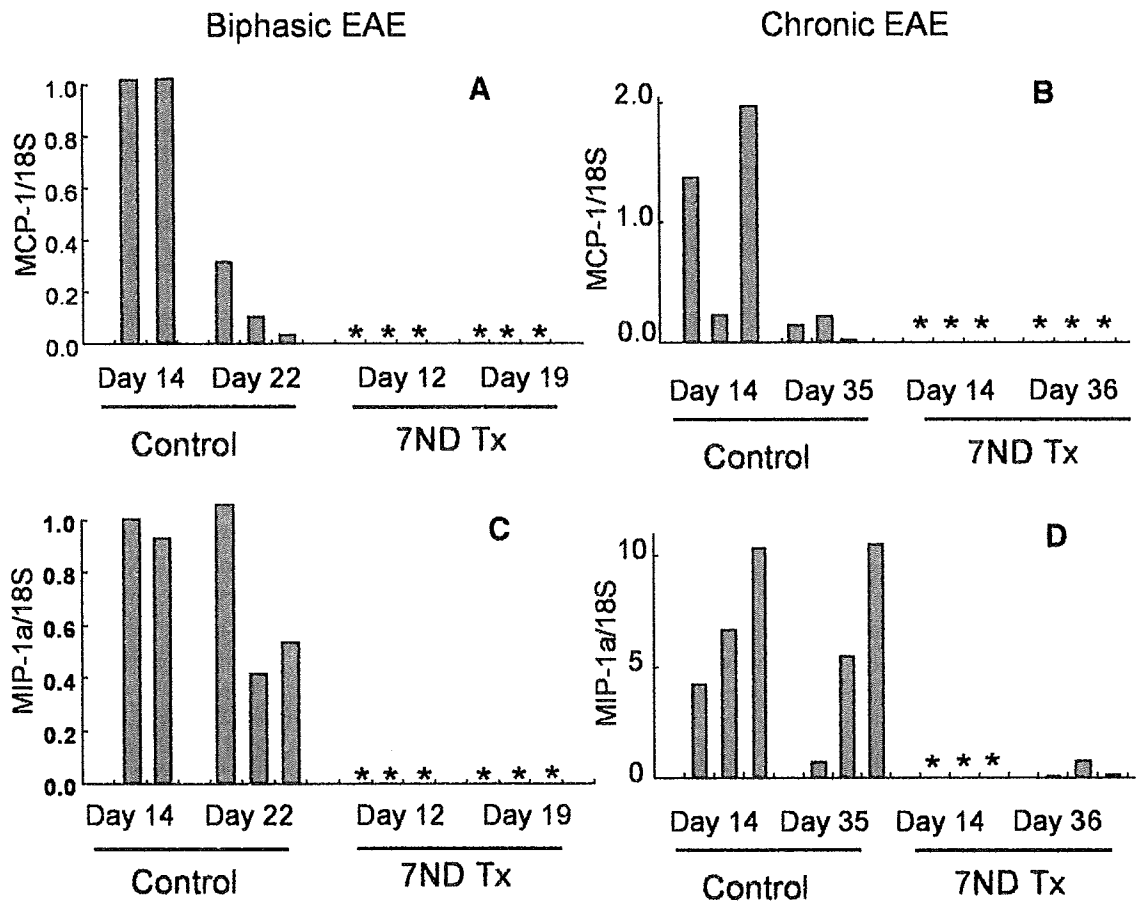

Fig. 3. Quantitation of chemokine mRNA. The levels of MCP-1/CCL2 (A and B) and MIP-1α/CCL3 (C and D) mRNA in the spinal cords of treated and control rats with biphasic (A and C) and chronic (B and D) EAE were determined with real-time PCR. Each bar represents a value from individual rats.

MCP-1/CCL2 (Fig. 3B) and MIP-1α/CCL3 (Fig. 3D) mRNA in the spinal cords of treated rats with chronic EAE were suppressed almost completely at the early and late stages of the disease.

3.5. Evaluation of anti-MBP and anti-MOG antibodies in biphasic and chronic EAE

We wished to know whether the therapeutic effects of 7ND administration are mediated by the downregulation of anti-neuroantigen antibodies. For this purpose, we determined the levels of anti-MBP and anti-MOG antibodies of treated and control rats with biphasic and chronic EAE. These antibodies were not detected in naive LEW, DA and LEW.1AV1 rats (data not shown). The results are illustrated in Fig. 4. As clearly shown, during the first attack of biphasic EAE (Days 11–12 in Fig. 4A and C), the levels of both anti-MBP and anti-MOG antibodies in treated animals were almost the same as those in control animals. During the relapse (Days 19–22 in Fig. 4A and C), anti-MOG (Fig. 4C), but not anti-MBP (Fig. 4A), antibodies were significantly lowered in the treated group compared with the control group. In treated and control rats with chronic EAE, the levels of anti-MBP (Fig. 4B) were almost under the detection level. Similarly, anti-MOG antibodies (Fig. 4D) were not affected by 7ND treatment although the disease was completely suppressed in the majority of rats. These findings suggested that amelioration of chronic EAE occurs without the downregulation of anti-neuroantigen antibodies. In acute EAE, the levels of anti-MBP antibodies remained low in both treated and control rats throughout the course of the disease (data not shown).

4. Discussion

Multiple sclerosis (MS) is thought to be an autoimmune disease characterized by the presence of multiple inflammatory and demyelinating lesions in the CNS (Bar-Or et al., 1999). Notably, there is profound heterogeneity in the clinical course and CNS lesions, suggesting that MS is a disease with heterogeneous pathomechanisms. Through careful observations of CNS tissues with actively demyelinating lesions, Lassmann and colleagues classified MS lesions into 4 patterns (Lassmann, 2004; Lucchinetti et al., 2000). Although their characterization of the MS lesions is highly suggestive of pathogenetic mechanisms of heterogeneous lesion formation in MS, there is limitation for further analysis since these results were obtained by the morphological examinations of autopsy materials.

In the present study, we induced three types of EAE using three antigens and three rat strains and tried to elucidate the pathomechanisms of the lesion formation in MS by examining various types of EAE clinically and pathologically. It should be

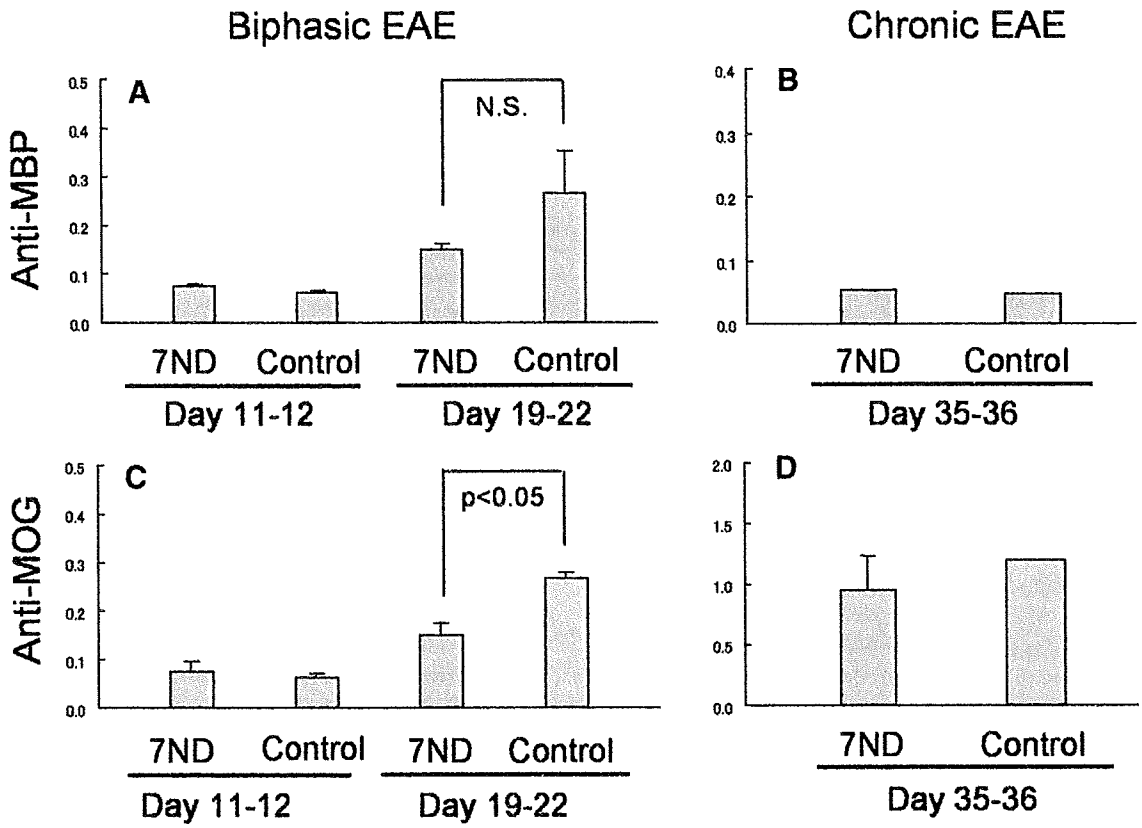

Fig. 4. Anti-MBP and anti-MOG antibodies in sera from rats with biphasic (A and C) and chronic (B and D) EAE. The levels of anti-MBP (A and B) and anti-MOG (C and D) antibodies in sera were determined by ELISA. The sera were collected on days 11–12 post-immunization (PI) during the first attack and days 19–22 PI during relapse of biphasic (A and C) and on days 35–36 and day 43 PI of chronic (B and D) EAE. Each bar represents the mean value (O.D.)±SD of three rats.

noted that such variations are unlikely to influence the results. This was because we only analyzed the role of T cells and macrophages in the lesion formation of each EAE and did not analyze variation-dependent factors such as the antigen specificity of T cells from three strains. For the analysis, we employed decoy chemokine, 7ND, which is a dominant inhibitor of MCP-1/CCL2. 7ND was reported to be a dominant negative inhibitor of MCP-1/CCL2 and not a competitive inhibitor for receptor binding because 7ND inhibited the non-cross-linked, but not the cross-liked, active form of MCP-1/CCL2 (Zhang and Rollins, 1995). As it was later demonstrated that glycosaminoglycan binding and oligomerization are essential for the in vivo activity of MCP-1/CCL2 (Lau et al., 2004; Proudfoot et al., 2003), 7ND may interfere with these processes. 7ND has been used, not only for in vitro studies, but also for the treatment of animal disease models including vascular diseases (Egashira, 2003; Egashira et al., 2000), arthritis (Gong et al., 1997) and pulmonary hypertension (Ikeda et al., 2002). To our knowledge, this is the first report showing that 7ND treatment is effective in preventing some subtypes of EAE. It is very interesting to note that 7ND treatment suppressed the relapse of biphasic EAE and chronic EAE, but not acute EAE and the first attack of biphasic EAE. It was previously reported that depletion of macrophages by liposomes containing dichloromethylene diphosphonate (Cl_2MDP) markedly suppressed the development of MBP-induced acute EAE in rats and mice (Huitinga et al., 1990; Tran et al., 1998). We have confirmed that Cl_2MDP, which was produced and administered exactly the same as that in the previous reports, suppressed acute EAE in Lewis rats (unpublished observation). The major difference in the immune conditions between Cl_2MDP and 7ND treatment was that 7ND treatment only inhibited macrophage migration and may minimally influence T cell functions, while liposome treatment would downregulate bioactive substances secreted by macrophages. This may be attributable to the difference in the outcome. Immunohistochemical examinations revealed that infiltrating macrophages in biphasic EAE lesions were substantially reduced in number by 7ND treatment and that chronic EAE lesions were completely normalized histologically. In contrast, the distribution and density of T cells in the lesion at the first attack of biphasic EAE were not different between the treated and control groups (Fig. 2) indicating that 7ND treatment does not interfere with T cell infiltration. These findings strongly suggest that the major effector cells are macrophages in the relapse of biphasic EAE and chronic EAE. With regard to the relapse of biphasic EAE, we previously reported that MCP-1/CCL2 was upregulated at this stage (Jee et al., 2002) and Kennedy et al. showed that administration of anti-MCP-1/CCL2 antibodies suppressed the relapse of mouse biphasic EAE (Kennedy et al., 1998). In addition, MCP-1/CCL-2-deficient mice developed significantly mild EAE (Huang et al., 2001). In the present study, we have demonstrated that anti-macrophage migration treatment by 7ND suppressed the relapse of biphasic EAE, indicating that MCP-1/CCL2 plays a key role of EAE relapse. It is less likely that 7ND administration induces the antibody

production because antibodies was not elevated in animals that had receive the therapeutic administration of plasmid DNAs as shown in a previous study (Matsumoto et al., 2004). In contrast to the relapse of biphasic EAE and chronic EAE, T cells may play a pivotal role in the development of acute EAE and the first attack of biphasic EAE. However, these findings do not exclude the possibility that T cells play a role in macrophage-dependent disease progression. Indeed, administration of anti-T cell monoclonal antibody suppressed the development of MOG-induced chronic EAE (our unpublished observation).

We determined the levels of macrophage-related chemokine mRNA in the spinal cord of rats during the relapse of biphasic and chronic EAE. Interestingly, the administration of 7ND, a dominant inhibitor of MCP-1/CCL2, suppressed both MCP-1/CCL2 and MIP-1α/CCL3 mRNA almost completely in the relapse of biphasic and chronic EAE. Although the precise mechanism by which the MCP-1/CCL2 inhibitor suppresses MIP-1α/CCL3 remains unknown, it was reported that 7ND suppresses a variety of cytokines and chemokines including IL-1β, RNATES, MIP-2 and IP-10 (Goser et al., 2005). Furthermore, pathological examinations revealed the marked decrease of macrophages in the lesions during the relapse of biphasic EAE (Table 3) and chronic EAE (Table 4). This may be attributable to general reduction of macrophage-related chemokines.

We also examined the levels of anti-MBP and anti-MOG antibodies in treated and control rats with three types of EAE. As clearly shown here, 7ND treatment ameliorated the clinical signs and pathology in some types of EAE without the downregulation of anti-neuroantigen antibodies. This finding suggests that 7ND exerts its function in a manner independent of the antibody production. However, this does not deny the role of anti-neuroantigen antibodies in chronic EAE and MS as demonstrated in previous studies (Lalive et al., 2006; Sakuma et al., 2004; von Budingen et al., 2002).

In summary, we have induced three different types of EAE in rats and treated them with the 7ND gene, a dominant inhibitor of MCP-1/CCL2, to elucidate the pathomechanisms of the lesion formation in EAE. Depending on the effect of the treatment in terms of the development of clinical signs and pathology, the lesion formation can be classified into two categories; i.e., T cell-dependent and macrophage-dependent lesion formations. These findings provide useful information to develop specific immunotherapies.

Acknowledgements

This study was supported in part by the Health and Labour Sciences Research Grants for Research on Psychiatric and Neurological Diseases and Mental Health and by Grants-in-Aid from the Japan Society for the Promotion of Science.

References

Agrawal, H.C., Burton, R.M., Fishman, M.A., Mitchell, R.F., Prensky, A.L., 1972. Partial characterization of a new myelin protein component. J. Neurochem. 19, 2083–2089.

Bar-Or, A., Oliveira, E.M., Anderson, D.E., Hafler, D.A., 1999. Molecular pathogenesis of multiple sclerosis. J. Neuroimmunol. 100, 252–259.

Bas, A., Forsberg, G., Hammarstrom, S., Hammarstrom, M.L., 2004. Utility of the housekeeping genes 18S rRNA, beta-actin and glyceraldehyde-3-phosphate-dehydrogenase for normalization in real-time quantitative reverse transcriptase-polymerase chain reaction analysis of gene expression in human T lymphocytes. Scand. J. Immunol. 59, 566–573.

Casado, V., Mallol, J., Bozal, J., 1988. Isolation and characterization of bovine brain myelin distribution of 5′-nucleotidase. Neurochem. Res. 13, 349–357.

Deibler, G.E., Martenson, R.E., Kies, M.W., 1972. Large scale preparation of myelin basic protein from central nervous tissue of several mammalian species. Prep. Biochem. 2, 139–165.

Egashira, K., 2003. Molecular mechanisms mediating inflammation in vascular disease: special reference to monocyte chemoattractant protein-1. Hypertension 41, 834–841.

Egashira, K., Koyanagi, M., Kitamoto, S., Ni, W., Kataoka, C., Morishita, R., Kaneda, Y., Akiyama, C., Nishida, K.I., Sueishi, K., Takeshita, A., 2000. Anti-monocyte chemoattractant protein-1 gene therapy inhibits vascular remodeling in rats: blockade of MCP-1 activity after intramuscular transfer of a mutant gene inhibits vascular remodeling induced by chronic blockade of NO synthesis. FASEB J. 14, 1974–1978.

Gong, J., Ratkay, L.G., Waterfield, J.D., Clark-Lewis, I., 1997. An antagonisit of monocyte chemoattractant protein 1 (MCP-1) inhibits arthritis in the MRL-*lpr* mouse model. J Exp. Med. 186, 131–137.

Goser, S., Ottl, R., Brodner, A., Dengler, T.J., Torzewski, J., Egashira, K., Rose, N.R., Katus, H.A., Kaya, Z., 2005. Critical role for monocyte chemoattractant protein-1 and macrophage inflammatory protein-1alpha in induction of experimental autoimmune myocarditis and effective anti-monocyte chemoattractant protein-1 gene therapy. Circulation 112, 3400–3407.

Huang, D.R., Wang, J., Kivisakk, P., Rollins, B.J., Ransohoff, R.M., 2001. Absence of monocyte chemoattractant protein 1 in mice leads to decreased local macrophage recruitment and antigen-specific T helper cell type 1 immune response in experimental autoimmune encephalomyelitis. J. Exp. Med. 193, 713–726.

Huitinga, I., Van Roonijen, N., De Groot, C.J.A., Uitdehaag, B.M.J., Dijkstra, C.D., 1990. Suppression of experimental allergic encephalomyelitis in Lewis rats after elimination of macrophages. J. Exp. Med. 172, 1025–1033.

Ikeda, Y., Yonemitsu, Y., Kataoka, C., Kitamoto, S., Yamaoka, T., Nishida, K., Takeshita, A., Egashira, K., Sueishi, K., 2002. Anti-monocyte chemoattractant protein-1 gene therapy attenuates pulmonary hypertension in rats. Am. J. Physiol. Heart Circ. Physiol. 283, H2021–H2028.

Jee, Y., Yoon, W.K., Okura, Y., Tanuma, N., Matsumoto, Y., 2002. Upregulation of monocyte chemoattractant protein-1 and CC chemokine receptor 2 in the central nervous system is closely associated with relapse of autoimmune encephalomyelitis in Lewis rats. J. Neuroimmunol. 128, 49–57.

Kennedy, K.J., Steir, R.M., Kunkel, S.L., Lukacs, N.W., Karpus, W.J., 1998. Acute and relapsing experimental encephalomyelitis are regulated by differential expression of the CC chemokines macrophage inflammatory protein-1α and monocyte chemotactic protein-1. J. Neuroimmunol. 92, 98–108.

Kim, G., Tanuma, N., Kojima, T., Kohyama, K., Suzuki, Y., Kawazoe, Y., Matsumoto, Y., 1998. CDR3 size spectratyping and sequencing of spectratype-derived T cell receptor of spinal cord T cells in autoimmune encephalomyelitis. J. Immunol. 160, 509–513.

Lalive, P.H., Menge, T., Delarasse, C., Della Gaspera, B., Pham-Dinh, D., Villoslada, P., von Budingen, H.C., Genain, C.P., 2006. Antibodies to native myelin oligodendrocyte glycoprotein are serologic markers of early inflammation in multiple sclerosis. Proc. Natl. Acad. Sci. U S A 103, 2280–2285.

Lassmann, H., 2004. Recent neuropathological findings in MS-implication for diagnosis and therapy. J. Neurol. Suppl. 4, IV/2–IV/5.

Lau, E.K., Paavola, C.D., Johnson, Z., Gaudry, J.P., Geretti, E., Borlat, F., Kungl, A.J., Proudfoot, A.E., Handel, T.M., 2004. Identification of the glycosaminoglycan binding site of the CC chemokine, MCP-1: implications for structure and function in vivo. J. Biol. Chem. 279, 22294–22305.

Lublin, F.D., Reingold, S.C., 1996. Defining the clinical course of multiple sclerosis: results of an international survey. Neurology 46, 907–911.

Lucchinetti, C., Brueck, W., Parisi, J., Scheithauer, B., Rodoriguez, M., Lassmann, H., 2000. Heterogeity of multiple sclerosis lesions: implication for the pathogenesis of demyelination. Ann. Neurol. 47, 707–717.

Matsumoto, Y., Fujiwara, M., 1987. The immunopathology of adoptively transferred experimental allergic encephalomyelitis (EAE) in Lewis rats.

Part 1. Immunohistochemical examination of developing lesion of EAE. J. Neurol. Sci. 77, 35–47.

Matsumoto, Y., Tsukada, Y., Miyakoshi, A., Sakuma, H., Kohyama, K., 2004. C protein-induced myocarditis and subsequent dilated cardiomyopathy: rescue from death and prevention of dilated cardiomyopathy by chemokine receptor DNA therapy. J. Immunol. 173, 3535–3541.

Matsumoto, Y., Sakuma, H., Miyakoshi, A., Tsukada, Y., Kohyama, K., Park, I., Naoyuki, T., 2005. Characterization of relapsing autoimmune encephalomyelitis and its treatment with decoy chemokine receptor gene. J. Neuroimmunol. 170, 49–61.

Ohmori, K., Hong, Y., Fujiwara, M., Matsumoto, Y., 1992. *In situ* demonstration of proliferating cells in the rat central nervous system during experimental autoimmune encephalomyelitis. Evidence suggesting that most infiltrating T cells do not proliferate in the target organ. Lab. Invest. 66, 54–62.

Proudfoot, A.E., Handel, T.M., Johnson, Z., Lau, E.K., LiWang, P., Clark-Lewis, I., Borlat, F., Wells, T.N., Kosco-Vilbois, M.H., 2003. Glycosaminoglycan binding and oligomerization are essential for the in vivo activity of certain chemokines. Proc. Natl. Acad. Sci. U S A 100, 1885–1890.

Sakuma, H., Kohyama, K., Park, I.K., Miyakoshi, A., Tanuma, N., Matsumoto, Y., 2004. Clinicopathological study of a myelin oligodendrocyte glycoprotein-induced demyelinating disease in LEW.1AV1 rats. Brain 127, 2201–2213.

Sospendra, M., Martin, R., 2005. Immunology of multipel sclerosis. Annu. Rev. Immunol. 23, 683–747.

Tran, E.H., Hoekstra, K., Van Rooijen, N., Dijkstra, C.D., Owens, T., 1998. Immune invasion of the central nervous system parenchyma and experimental allergic encephalomyelitis, but not leukocyte extravasation from blood, are prevented in macrophage-depleted mice. J. Immunol. 161, 3767–3775.

van der Goes, A., Boorsma, W., Hoekstra, K., Montagne, L., De Groot, C.J.A., Dijkstra, C.D., 2005. Determination of the sequential degradation of myelin protein by macrophages. J. Neuroimmunol. 161, 12–20.

von Budingen, H.C., Hauser, S.L., Fuhrmann, A., Nabavi, C.B., Lee, J.I., Genain, C.P., 2002. Molecular characterization of antibody specificities against myelin/oligodendrocyte glycoprotein in autoimmune demyelination. Proc. Natl. Acad. Sci. U S A 99, 8207–8212.

Zhang, Y., Rollins, B.J., 1995. A dominant negative inhibitor indicates that monocyte chemoattractant protein 1 functions as a dimer. Mol. Cell Biol. 15, 4851–4855.

Zhang, Y.J., Rutledge, B.J., Rollins, B.J., 1994. Structure/activity analysis of human monocyte chemoattractant protein-1 (MCP-1) by mutagenesis. Identification of a mutated protein that inhibits MCP-1-mediated monocyte chemotaxis. J. Biol. Chem. 269, 15918–15924.

The American Journal of Pathology, Vol. 170, No. 1, January 2007

DOI: 10.2353/ajpath.2007.060544

Cardiovascular, Pulmonary and Renal Pathology

B-Cell Epitope Spreading Is a Critical Step for the Switch from C-Protein-Induced Myocarditis to Dilated Cardiomyopathy

Yoh Matsumoto, Il-Kwon Park, and Kuniko Kohyama

From the Department of Molecular Neuropathology, Tokyo Metropolitan Institute for Neuroscience, Tokyo, Japan

Repeated inflammation in the heart is one of the initiation factors of dilated cardiomyopathy (DCM). In a previous study, we established a new animal model for DCM by immunization of rats with recombinant cardiac C-protein fragment 2 (CC2). The present study examined factors involved in the development of DCM. Analysis using overlapping peptides revealed that the major carditogenic epitope resides only in the residue 615–647 [CC2 peptide 12 (CC2P12)]. However, immunization with CC2P12 induced moderate inflammation without subsequent DCM. CDR3 spectratyping analysis of the T-cell repertoire demonstrated that Vβ4-positive T cells were preferentially expanded in both CC2- and CC2P12-immunized rats. Although there was no significant difference in the T-cell characteristics, examinations of the B-cell epitope revealed that marked epitope spreading occurred in CC2-immunized but not CC2P12-immunized rats from 4 weeks after immunization. Consistent with this finding, immunization with CC2P12 and simultaneous transfer of anti-peptide antisera induced significantly more severe inflammation and fibrosis than CC2P12 immunization alone. However, the transfer of the antisera without CC2P12 immunization did not induce any pathology. These findings suggest that T-cell activation and B-cell epitope spreading in the CC2 molecule is a key step for the switch from myocarditis to the development of DCM. ***(Am J Pathol 2007, 170:43–51; DOI: 10.2353/ajpath.2007.060544)***

Dilated cardiomyopathy (DCM) is a serious and frequently fatal disorder and is a common cause of heart failure. The majority of DCM is sporadic, and mostly virus-induced immune mechanisms are suspected.[1] Because the heart biopsy sometimes demonstrates the presence of inflammation, several immunosuppressive therapies have been tried to improve the status of DCM.[2–4] However, significant progress has not been made, although these therapies have shown some improvements of the disease. Difficulties in finding effective therapies are mainly based on the fact that the pathogenesis of DCM is still poorly understood. The establishment of a suitable animal model that mimics human DCM and elucidation of pathogenesis of DCM will provide useful information for the development of effective therapies.

In a previous study, we demonstrated that cardiac C-protein, one of the myosin-binding proteins, induced severe experimental autoimmune carditis (EAC) and subsequent DCM in Lewis rats.[5] Seventy-five percent of rats immunized with C-protein died by day 50, and all of the survivors developed DCM. Furthermore, it was revealed that cytokines and chemokines produced by T cells and macrophages were up-regulated in the heart lesions, mainly during the inflammatory phase of EAC. These findings suggest that pathogenic T cells and possibly B cells play an important role in the development of EAC and subsequent DCM.

In the present study, we first examined the carditogenic epitopes that reside in the cardiac C-protein fragment 2 (CC2) (corresponding to amino acid residues 317–647). Using overlapping peptides, we found that only peptide 12 (CC2P12) possessed the carditis-inducing ability in the CC2 molecule. Interestingly, CC2P12 induced nonfatal moderate EAC and did not develop DCM. Analysis of clonally expanded T cells in CC2- and CC2P12-immunized rats demonstrated that there was no significant difference between the two groups. In contrast, CC2-immunized rats exhibited marked B-cell epitope spreading 4 weeks after immunization and afterward, whereas CC2P12-immunized rats raised antibodies only against CC2P12 and CC2. Based on these

Supported in part by grants-in-aid from the Japan Society for the Promotion of Science.

Accepted for publication September 14, 2006.

Address reprint requests to Yoh Matsumoto, Department of Molecular Neuropathology, Tokyo Metropolitan Institute for Neuroscience, Musashidai 2-6, Fuchu, Tokyo 183-8526, Japan. E-mail: matyoh@tmin.ac.jp.

Table 1. Amino Acid Sequences of Synthetic Peptides Encompassing CC2 Used in the Study

Peptide	Residue	Sequence
P1	317–348	AEEDVWEILRQAPPSEYERIAFQYGVTDLRGM
P2	344–375	DLRGMLKRLKGMRRDEKKSTAFQKKLEPAYQV
P3	371–402	PAYQVSKGHKIRLTVELADHDAEVKWLKNGQE
P4	398–429	KNGQEIQMSGSKYIFESIGAKRTLTISQCSLA
P5	425–456	QCSLADDAAYQCVVGGEKCSTELFVKEPPVLI
P6	452–483	PPVLITRPLEDQLVMVGQRVEFECEVSEEGAQ
P7	479–510	EEGAQVKWLKDGVELTREETFKYRFKKDGQRH
P8	506–537	DGQRHHLIINEAMLEDAGHYALCTSGGQALRE
P9	533–564	QALRELIVQEKKLEVYQSIADLMVGAKDQAVF
P10	560–591	DQAVFKCEVSDENVRGVWLKNGKELVPDSRIK
P11	587–619	DSRIKVSHIGRVHKLTIDDVTPADEADYSFVPE
P12	615–647	SFVPEGFACNLSAKLHFMEVKIDFVPRQEPPKI

C-protein fragment 2 encompasses amino acid 317–647 residues of human cardiac C-protein.

findings, we performed transfer experiments and demonstrated that both activation of T cells and anti-peptide antibody elevation are required for the initiation and subsequent progression of the disease. The present study strongly suggests that B-cell epitope spreading is an essential step for the switch from myocarditis to DCM.

Materials and Methods

Animals and Proteins

Lewis rats were purchased from SLC Japan (Shizuoka) and bred in our animal facility. Seven- to 11-week-old male and female rats were used.

Preparation of Recombinant C-Protein Fragments and Synthetic Peptides

The preparation of recombinant C-protein was precisely described previously.[5] Polymerase chain reaction (PCR) products corresponding to fragments 1, 2, 3, and 4 were inserted into a cloning vector, pCR4 Blunt-TOPO in the Zero Blunt TOPO kit (Invitrogen, Groningen, The Netherlands), and clones with correct sequences were subcloned into an expression vector, pQE30 (Qiagen, Tokyo, Japan). Then, recombinant C-protein fragments produced in transformed *Escherichia coli* were isolated under denaturing conditions and purified using Ni-NTA Agarose (Qiagen).

Synthetic peptides encompassing CC2, designated as CC2P1-CC2P12 (Table 1), were synthesized using a peptide synthesizer (Shimadzu, Kyoto, Japan). All of the peptides used in this study were >90% pure as determined and were purified if necessary using HPLC.

Conjugation of CC2P12 with KLH

To increase immunogenicity of CC2P12, the peptide was conjugated with keyhole limpet hemocyanin (KLH; Wako, Tokyo, Japan) as described previously.[6] KLH (in 0.083 mol/L sodium phosphate, 0.9 mol/L NaCl, and 0.1 mol/L ethylenediamine tetraacetic acid, pH 7.2) and *m*-maleimidobenzoyl-*N*-hydrosuccinimide ester in dimethyl sulfoxide (MBS; Pierce, Chicago, IL) at concentrations of 10 and 20 mg/ml, respectively, were incubated at a ratio of 10:1 for 1 hour at room temperature. Then, excess MBS was removed on a HiTrap desalting column (Amersham Biosciences, Tokyo, Japan). Finally, the KLH-CC2P12 complex was formed by incubating MBS-KLH with CC2P12 for 2 hours at room temperature.

EAC Induction and Tissue Sampling

Lewis rats were immunized once on day 0 with the indicated antigen with complete Freund's adjuvant (CFA) (2.5 mg/ml *Mycobacterium tuberculosis*) in the hind foot pads. At the time of immunization, rats received an intraperitoneal injection of 2 μg of pertussis toxin (PT; Seikagaku Corp., Tokyo, Japan). The numbers of rats used for experiments are shown in the footnotes of tables and the figure legends. Histological and immunohistochemical examinations were performed at the indicated time points using frozen and paraffin-embedded sections of the heart. Although evaluation of EAC and DCM was mainly based on histological examinations (see below), clinical score was also recorded: grade 1, dyspnea; grade 2, dyspnea plus ruffling of fur; and grade 3, moribund condition or death.

Histological Grading of Inflammatory Lesions and Immunohistochemistry

EAC inflammatory lesions were evaluated using hematoxylin and eosin (H&E)-stained sections according to the following criteria: grade 1, rare focal inflammatory lesions; grade 2, multiple isolated foci of inflammation frequently associated with pericarditis; grade 3, diffuse inflammation involving the outer layer of the muscle; grade 4, grade 3 plus focal transmural inflammation; and grade 5; diffuse inflammation with necrosis. CC2 immunization induced pericarditis that was frequently associated with pericardial and pleural effusion. However, we did not include the findings in the scores because the above grading system covered the whole range of mild to severe EAC. The extent of fibrosis revealed by Azan staining was graded into five categories: grade 1, rare scattered foci of fibrosis; grade 2, multiple isolated foci of fibrosis; grade 3, fibrosis involving the outer layer of the

muscle; grade 4, grade 3 plus partial transmural fibrosis; and grade 5, diffuse fibrosis.

Establishment of T-Cell Lines and the Proliferative Assay

CC2- or CC2P12-specific T-cell lines were established from draining (popliteal) lymph node cells taken from CC2- or CC2P12-immunized rats by cycle stimulations with CC2 or CC2P12 in the presence of mitomycin C-treated thymocytes as antigen-presenting cells. Between antigen stimulations, T cells were propagated in culture medium containing 5% Con A supernatant.

Proliferative responses of lymph node cells were assayed in microtiter wells by the uptake of [^{3}H]thymidine. After being washed with phosphate-buffered saline, lymph node cells (2×10^5 cells/well) were cultured with the indicated concentrations of CC2 or CC2 peptides for 3 days, with the last 18 hours in the presence of 0.5 μCi of [^{3}H]thymidine (Amersham Pharmacia Biotech, Tokyo, Japan). In some experiments, the proliferative responses of CC2- or CC2P12-specific T-cell lines (3×10^4 cells/well) were assayed in the presence of the antigens and antigen-presenting cells (5×10^5 cells/well). The cells were harvested on glass-fiber filters, and the label uptake was determined using standard liquid scintillation techniques.

CDR3 Spectratyping

CDR3 spectratyping was performed as described previously.[7,8] In brief, PCR products were added to an equal volume of formamide/dye loading buffer and heated at 94°C for 2 minutes. The amplified PCR products were electrophoresed on polyacrylamide sequencing gels, and the fluorescence-labeled DNA profile on the gels was directly recorded using an FMBIO fluorescence image analyzer (Hitachi, Yokohama, Japan). The presence or absence of contaminations of the reagents used in PCR was examined every 10 PCR analyses by performing PCR without the templates. When contaminations were present, all reagents used and the results obtained during the period were discarded.

ELISA

The levels of anti-CC2 and anti-CC2 peptide antibodies were measured using the standard ELISA test. Recombinant CC2 and CC2P1-P12 (10 μg/ml) were coated onto microtiter plates, and serially diluted sera from normal and immunized animals were applied. After washing, appropriately diluted horseradish-conjugated anti-rat IgG, IgG1, or IgG2a was applied. The reaction products were then visualized after incubation with the substrate. The absorbance was read at 450 nm.

Generation of Polyclonal Antibodies Against CC2 and CC2 Peptides

Polyclonal antibodies against CC2 and CC2 peptides were raised by immunizing rats with the antigens/CFA four times on a weekly basis. Sera were obtained 1 week after the last immunization, and ammonium sulfate-precipitated preparations were used for the transfer experiments. The presence of antibodies against the indicated antigens was confirmed by ELISA.

Statistical Analysis

Unless otherwise indicated, Student's *t*-test or Mann-Whitney's *U*-test was used for the statistical analysis.

Results

Autoimmune Carditis-Inducing Ability of Recombinant C-Protein and Synthetic Peptides

As reported in our previous study,[5] recombinant CC2 (amino acid residues 317–647 of human cardiac C-protein) possessed the strongest carditogenic activity among four recombinant proteins encompassing the entire molecule. In the present study, we prepared 12 overlapping synthetic peptides (Table 1) covering the CC2 molecule and examined their carditis-inducing ability. As shown in Table 2, we first screened all of the peptides using the peptide mixtures (groups A through D). Only mixture 4 containing peptides 10, 11, and 12 at 100 μg of each peptide (CC2P10 to -P12) induced EAC in all of the immunized rats (group D), whereas mixtures 1, 2, and 3 induced mild EAC in one of three rats (groups A through C). Then, we tested the carditogenicity of each peptide in mixture 4 and found that only peptide 12 (CC2P12) possessed a carditis-inducing ability (group G). However, it should be noted that compared with CC2, both inflammation and fibrosis induced with CC2P12 were significantly milder as estimated on day 17 and 6 weeks after immunization (group G versus group I). Because immunization with 300 μg of CC2P12 did not differ to 100 μg of CC2P12 immunization in terms of the histological severity, the pooled data are shown in Table 2. In addition, CC2P12-immunized rats did not develop DCM at 6 weeks postimmunization (PI) (see below). Another important aspect was the survival rate. As shown in Figure 1, 75% of the rats immunized with CC2 died of cardiac failure by day 50 PI. In sharp contrast, all of the rats immunized with CC2P12 had survived by day 50. Furthermore, CC2P12 was conjugated with KLH to increase the immunogenicity, and rats were immunized with the conjugate. However, this procedure did not augment the carditis-inducing ability of CC2P12 (group H). In an additional experiment, we immunized rats with a mixture of P1, P5, P8, P11, and P12, but the histological score was not significantly different from that of P12-immunized rats (data not shown). Collectively, these findings suggest that substances induced after CC2P12 immunization lack

Table 2. Histological Severities of EAC Induced by Immunization with the Peptide Mixtures, Synthetic Peptides, and Recombinant CC2*

Group	Antigen	Sampling	Incidence	Inflammation	Fibrosis
A	Mix 1 (P1 to P3)	3 weeks	1/3	0.7 ± 0.7	0
B	Mix 2 (P4 to P6)	3 weeks	1/3	0.3 ± 0.3	0
C	Mix 3 (P7 to P9)	3 weeks	1/3	0.2 ± 0.2	0
D	Mix 4 (P10 to P12)	3 weeks	3/3	2.5 ± 1.2	0
E	P10	Day 17	0/3	0†	0
F	P11	Day 17	1/3	0.2 ± 0.2†	0
G	P12	Day 17	4/4	2.0 ± 0.4†	0
		6 weeks	6/6	1.8 ± 0.4†	1.8 ± 0.6‡
H	P12-KLH	4 weeks	2/3	0.7 ± 0.3	0.7 ± 0.3
		6 weeks	3/3	1.3 ± 0.3†	0.8 ± 0.4‡
I	CC2	Day 17	5/5	4.1 ± 0.4†	1.5 ± 0.4
		6 weeks	6/6	3.8 ± 0.2†	4.1 ± 0.2‡

*Lewis rats were immunized once with mixtures 1, 2, 3, and 4 that had consisted of peptides 1 to 3, 4 to 6, 7 to 9, and 10 to 12, respectively (100 μg of each peptide), in CFA in the foot pads along with intraperitoneal injection of pertussis toxin (2 μg). Because mix 4 showed carditogenicity, each peptide in the mixture (P10, P11, and P12) was tested in a similar manner. For comparison, the results obtained with recombinant C-protein fragment 2 are also shown. The denominators in the incidence column represent the number of rats used for each experiment.

†Analysis of variance and multiple comparison (Scheffe's F-test) were performed, and significant differences were noted in the following combinations: P10 versus CC2, $P = 0.002$; P11 versus CC2, $P = 0.0001$; P12 versus CC2, $P = 0.008$ on day 17; P12 versus CC2, $P = 0.003$; P12-KLH versus CC2, $P = 0.003$ at 6 weeks.

‡Significant differences were noted in the following combinations: P12 versus CC2, $P = 0.011$; P12-KLH versus CC2, $P = 0.004$ at 6 weeks.

some aggravation factors for EAC/DCM induced by immunization with CC2.

Figure 2 depicts normal histology of the heart (A, D, G, and J) and pathology of EAC induced by CC2 (B, E, H, and K) and CC2P12 (C, F, I, and L). At 2 weeks PI, when EAC was at the acute inflammatory stage, the hearts taken from CC2-immunized rats showed marked hypertrophy (Figure 1B), whereas the hearts from CC2P12-immunized rats showed slight enlargement (Figure 1C). We measured the long and short axes of the middle portion of normal, CC2-immunized, and CC2P12-immunized rats and calculated the heart area at this level. As shown in Table 3, there were significant differences between normal and CC2-immunized rats ($P = 0.01$) and between CC2- and CC2P12-immunized rats ($P = 0.005$), indicating that the hearts from CC2-immunized rats showed marked hypertrophy. In contrast, there was no significant difference between the normal and CC2P12-immunized groups. H&E (Figure 2, E and F) and azan (Figure 2, H and I) stainings showed that compared with CC2-induced EAC (Figure 2, E and H), both inflammation and fibrosis were mild (Figure 2, F and I). In sections immunostained for macrophages, there was extensive and diffuse macrophage infiltration in CC2-induced EAC (Figure 2K), whereas macrophage infiltration in CC2P12-induced EAC was mild and focal (Figure 2L). B-cell infiltration was absent in both types of EAC (data not shown).

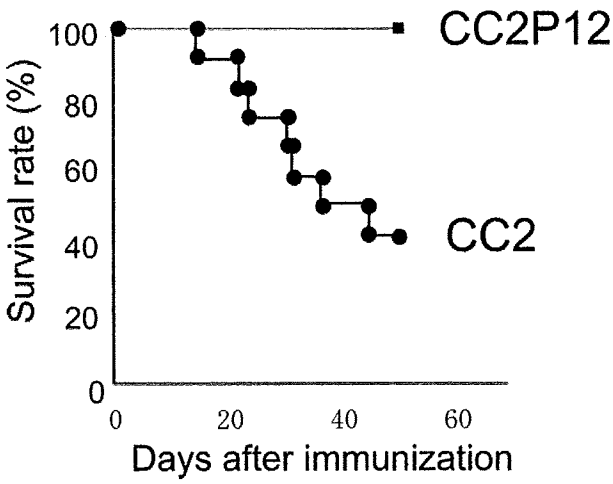

Figure 1. The survival rate of rats immunized with recombinant CC2/CFA or CC2P12/CFA with the intraperitoneal injection of pertussis toxin. Seventy-five percent of rats immunized with CC2 died between days 15 and 49 PI, whereas all of the rats immunized with CC2P12 survived during the observation period.

Characterization of Pathogenic T Cells

We next tried to determine whether a carditogenic peptide, CC2P12, contains an immunodominant or cryptic T-cell epitope. The representative results of three experiments are shown in Figure 3, A and B. When CC2 was immunized, the draining lymph node cells responded vigorously to CC2 but not to all of the overlapping peptide (P1 to P12 in Figure 3A). Similar experiments were performed using CC2-specific T-line cells after four to five cycles of antigen stimulation, and essentially the same results were obtained (data not shown). After CC2P12 immunization, lymph node cells responded well to CC2P12 and also to CC2 to a lesser extent (Figure 3B). These findings suggest that CC2P12 is processed and presented to T cells from CC2P12-immunized rats but is a cryptic epitope in the CC2 molecule for T cells from CC2-immunized rats.

In a previous study, we showed with CDR3 spectratyping analysis that in cardiac myosin-induced EAC, Vβ8.2 and Vβ10 TCR were clonally expanded in the inflamed heart and that Vβ8.2- and Vβ10-targeted immunotherapy was effective in ameliorating the severity of EAC.[7] We performed a similar analysis to characterize the nature of clonally expanded T cells in the heart with C-protein-induced EAC. The representative profiles are depicted in Figure 3, C and D, and all of the results are

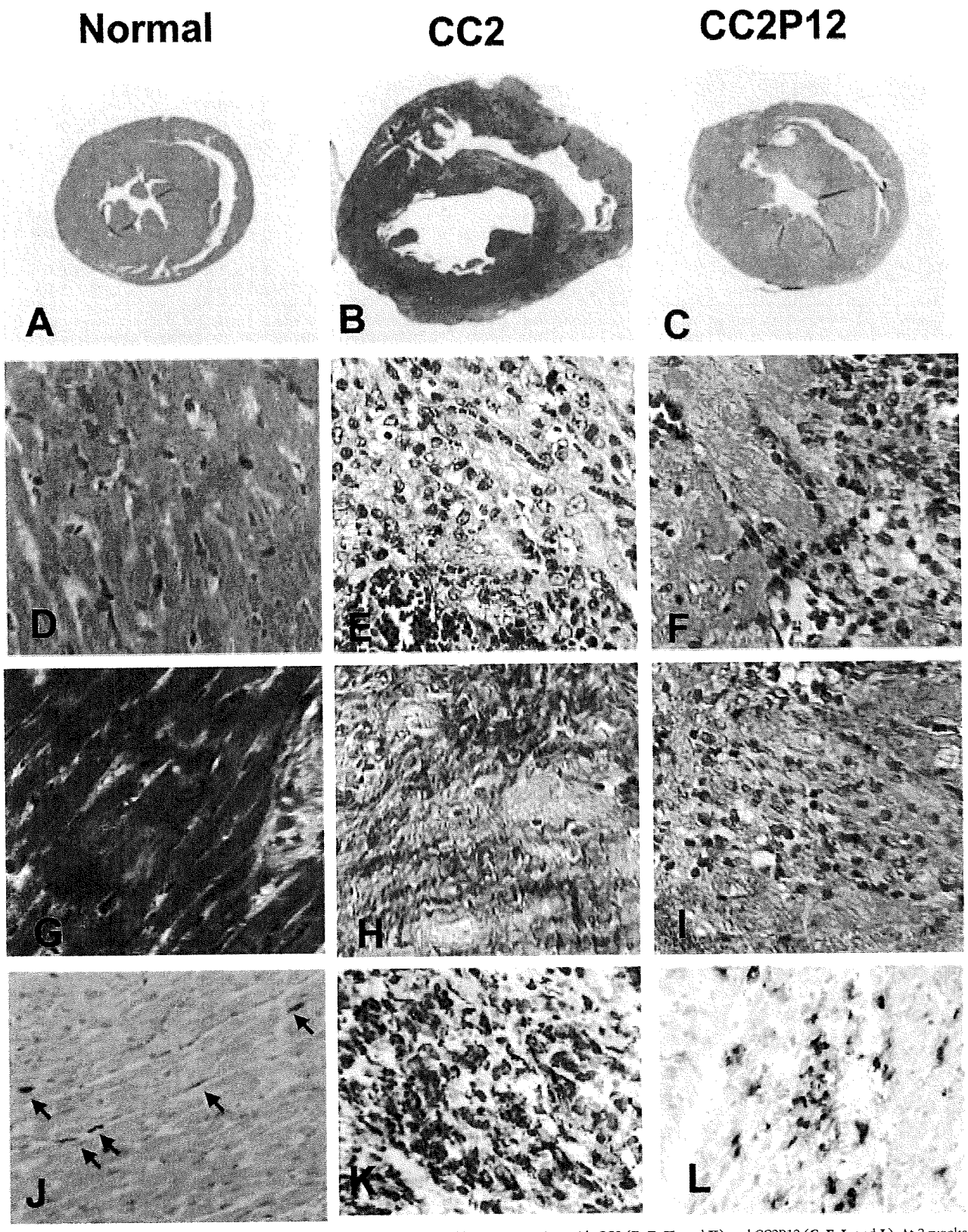

Figure 2. Normal histology (**A**, **D**, **G**, and **J**) and pathology of EAC induced by immunization with CC2 (**B**, **E**, **H**, and **K**) and CC2P12 (**C**, **F**, **I**, and **L**). At 2 weeks PI, when EAC was at the acute inflammatory stage, the hearts taken from CC2-immunized rats showed marked hypertrophy (**B**) compared with the normal heart (**A**), whereas the hearts from CC2P12-immunized rats showed only slight enlargement (**C**). H&E (**E** and **F**) and azan (**H** and **I**) stainings showed that compared with CC2-induced EAC (**E** and **H**), both inflammation and fibrosis of the heart were mild in CC2P12-immunized rats (**F** and **I**). In sections immunostained for macrophages, there was extensive and diffuse macrophage infiltration in CC2-induced EAC (**J**), whereas macrophage infiltration in CC2P12-induced EAC was mild and focal (**K**). **A–C:** H&E staining; the photographs were taken at the same magnification. **D–F:** H&E staining, ×240. **G–I:** Azan staining, ×240. **J–L:** ED1 staining, ×240.

Table 3. Measurements of Hearts under Normal and Diseased Conditions*

Condition	No. of rats examined	Diameter (mm)		Estimated area of hearts (mm^2)†
		Long axis	Short axis	
Normal	3	0.83 ± 0.10	0.72 ± 0.12	0.47 ± 0.14‡
CC2	6	1.20 ± 0.19	0.97 ± 0.08	0.91 ± 0.19‡
CC2P12	6	0.91 ± 0.08	0.80 ± 0.11	0.58 ± 0.13‡

*Rats were immunized once with CC2 or CC2P12, and the hearts were taken at 6 weeks after immunization. The long and short axes of the diameter were measured at the middle portion of the hearts. The hearts from CC2P12-immunized rats were measured before and after fixation, and those from normal and CC2-immunized rats were measured only after fixation. Because there was no significant change before and after fixation, all the values shown in the table are those measured after fixation.

†The heart area was calculated as long axis/2 × short axis × 3.14.

‡Significant differences were noted between normal and CC2-immunized rats (P = 0.01) and between CC2- and CC2P12-immunized rats (P = 0.005). However, there was no significant difference between normal and CC2P12-immunized rats.

summarized in Figure 3E. Infiltrating T cells in the heart of CC2-immunized rats on day 25 PI showed Vβ3 and Vβ4 expansion (Figure 3C, arrows), and those of CC2P12-immunized rats on day 17 PI showed Vβ4, Vβ8.6, and Vβ17 expansion (Figure 3D, arrows). The longitudinal study of CC2-immunized rats revealed interesting findings. On day 9 PI, T cells infiltrating the heart were rather

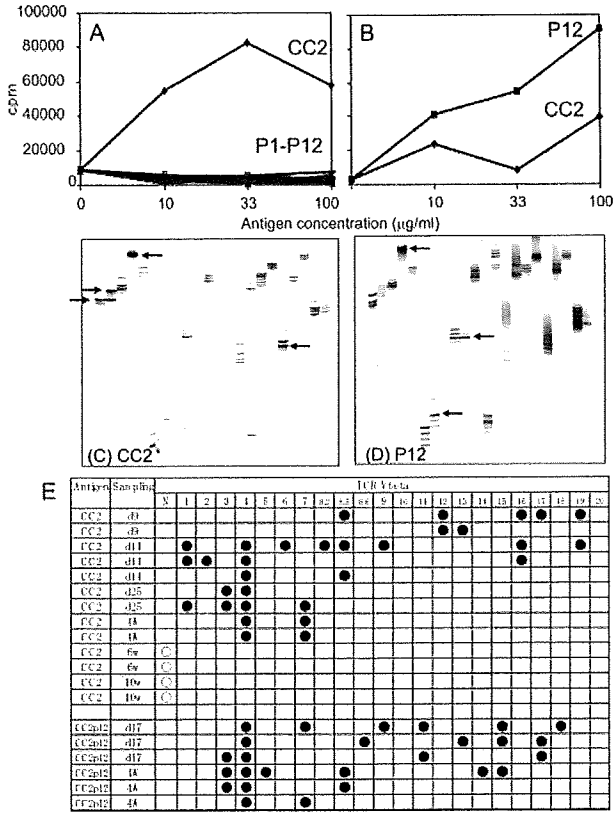

Figure 3. A and **B:** The proliferative responses of lymph node cells taken from CC2-immunized (**A**) and CC2P12-immunized (**B**) rats on day 12 PI. Lymph node cells (2×10^5 cells/well) were cultured with the indicated antigen for 72 hours, with the last 18 hours in the presence of [^{3}H]thymidine. The cells were harvested on glass-fiber filters, and the label uptake was determined using standard liquid scintillation techniques. Each symbol represents the mean value of triplicate assays, and SEMs were within 10% of the mean values. **C** and **D:** CDR3 spectratyping profiles of heart-infiltrating T cells taken from CC2-immunized (**C**) and CC2P12-immunized (**D**) rats. Marked spectratype expansions are indicated by **arrows**. **E:** Summary of the results of CDR3 spectratyping of T cells in the hearts from CC2- and CC2P12-immunized rats. Each line represents the result obtained from one rat. Closed circles represent Vβ clonal expansion. N, the normal spectratype pattern; w, weeks.

heterogonous, and no particular Vβ expansion was noted (Figure 3E). In contrast, between days 14 and 28 PI when the inflammatory lesion reached at the maximal level,[5] Vβ4 expansion was detected in all of the cases examined. Other Vβs such as Vβ1, -7, -8.5, and -16 were expanded in one-half of the cases. Interestingly, T cells found in the heart at the later stage (6 and 10 weeks), when there was extensive fibrosis, showed the normal spectratype pattern (Figure 3E). These findings suggested that infiltrating T cells showing oligoclonal expansion play an important role in the development of EAC lesions (see the results of the transfer experiments below). However, T cells found at the later stage may be less involved in the disease progression. CDR3 spectratyping analysis of heart-infiltrating T cells of CC2P12-immunized rats was performed on day 17 and at 4 weeks PI and revealed that there was Vβ4 expansion in all of the cases examined. Taken together, Vβ4-positive T cells appear to play an important role in lesion formation in both CC2- and CC2P12-induced EAC, and there was no significant difference in the T-cell characteristics between the two groups.

Characterization of Pathogenic B Cells and Anti-C-Protein Antibodies

As shown in Table 2 and Figure 2, CC2P12-immunized rats showed mild to moderate EAC without subsequent DCM. Moreover, unlike CC2-induced EAC, CC2P12-induced EAC was not fatal. These findings suggest that there are factors in CC2, but not in CC2P12, that aggravate EAC and induce DCM. Because we did not find clear differences between CC2- and P12-reactive T cells in the clonality analysis, we next examined the nature of antibodies raised by CC2 (Figure 4A) and CC2P12 (Figure 4B) immunization. From 1 to 12 weeks PI, sera were collected from CC2-immunized rats, and the levels of antibodies against CC2 and CC2P1 to -P12 were determined by ELISA (Figure 4A). At the early stage (1 to 3.5 weeks), only anti-CC2 antibodies were elevated in CC2-immunized rats. Then, anti-P8 and anti-P11 antibodies rose between 4 and 6 weeks, and some others showed at a high level thereafter. In one case examined at 12 weeks PI (4335 in Figure 4A), antibodies against all of the peptides were detected. This finding clearly showed that there was B-cell epitope spreading in CC2-immunized

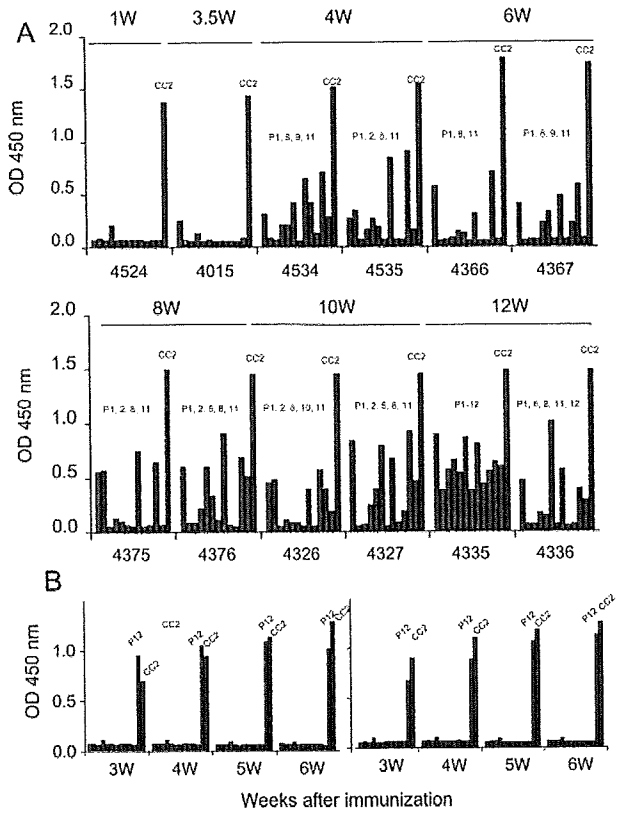

Figure 4. The kinetics of anti-CC2 and anti-CC2 peptide antibodies in CC2-immunized (**A**) and CC2P12-immunized (**B**) rats. **A:** The levels of anti-CC2 and anti-CC2 peptide antibodies were determined using ELISA. Recombinant CC2 and CC2P1-P12 (10 μg/ml) were coated onto microtiter plates, and diluted sera from CC2-immunized rats were applied. After washing, horseradish peroxidase-conjugated anti-rat IgG was allowed to react. The reaction products were then visualized after incubation with the substrate. The absorbance was read at 450 nm. **B:** The kinetics of anti-CC2 and anti-CC2 peptide antibodies in CC2P12-immunized rats. During the observation period, only anti-CC2P12 and anti-CC2 antibodies were elevated.

rats. Because this phenomenon was detected in the peripheral blood and there was no B-cell infiltration in the heart (data not shown), B-cell epitope spreading would take place in the lymphoid organ. In sharp contrast, in CC2P12-immunized rats, only antibodies against CC2P12 and CC2 were recognized in all of the rats examined by 6 weeks PI (Figure 4B).

CC2P12 Immunization and Cotransfer of Anti-CC2 or CC2 Peptide Antibodies Elicited Severe EAC

We further tried to identify factors that are responsible for the development of full-blown EAC and subsequent DCM. We already obtained the following findings. First, although CC2P12 was the sole carditis-inducing peptide in the CC2 molecule, CC2P12 induced relatively mild EAC without subsequent DCM. Second, there was no significant difference in the T-cell specificity between CC2-immunized and CC2P12-immunized rats. Finally, CC2-immunized rats showed marked intramolecular epitope spreading in the antibody production, whereas CC2P12-immunized rats developed antibodies that reacted with the immunizing antigen and the CC2 molecule. These findings raised the possibility that the generation of CC2-reacting T cells and generation of antibodies against various parts of the CC2 molecule are essential for full-blown EAC and subsequent DCM.

To test this possibility, we performed transfer experiments using various types of T cells and antibodies. The results are summarized in Table 4. Adoptive transfer of spleen and lymph node cells induced mild EAC in the recipients, whereas adoptive transfer of CC2-specific T-line cells did not elicit inflammation (Table 4, groups A and B). This finding suggests that not only T cells but also B cells are required for the development of inflammation in the heart. Cotransfer of anti-CC2 or anti-CC2P1–12 antisera after CC2P12 immunization aggravated both inflammation (Table 4, group D versus F, $P = 0.03$; group E versus F, $P = 0.005$) and fibrosis (Table 4, group D versus F, $P = 0.049$; group D versus F, $P = 0.01$) of EAC. There was no significant difference in the carditis-exacerbating ability between anti-CC2P1–12 and anti-CC2 antisera (Table 4, group D versus E). It should be noted that the transfer of anti-CC2 antisera alone did not induce EAC at all (group G). These findings strongly suggest that T cells are required for the initiation of inflammation in the heart and that anti-CC2 antibodies aggravate both inflammation and fibrosis.

Discussion

DCM is a serious problem for patients with heart failure because the disease progresses irreversibly and often ends in death. To develop effective therapies, it is essential to elucidate the pathomechanisms of the development of DCM. However, there are few good experimental models for DCM. In a previous study, we succeeded in inducing severe EAC with a high fatality rate and subsequent DCM in survivors by immunizing Lewis rats with cardiac C-protein.[5] This animal model is useful not only for the elucidation of the pathomechanisms of DCM but also for the development of effective immunotherapies.[5]

In the present study, we first tried to determine the carditis-inducing epitopes in the CC2 molecule and found that only peptide 12 (CC2P12), covering the residues 615–647, contains carditogenic epitope(s). Interestingly, immunization with CC2P12 induced moderate EAC but did not lead to subsequent DCM. Here, we demonstrated in a C-protein-induced animal model that B-cell epitope spreading occurred in CC2-immunized rats with DCM but not in CC2P12-immunized rats without DCM and that elevation of antibodies against various parts of the CC2 molecule is essential for the induction of more severe inflammation and fibrosis. However, it should be noted that activation of pathogenic T cells as demonstrated by CDR3 spectratyping is essential for the initiation of lesion formation because adoptive transfer of anti-CC2 antisera alone did not induce pathology at all.

Epitope spreading was first described in detail by Lehmann et al[9] as a key process for the development of chronic autoimmune encephalomyelitis. Initially, T-cell

Table 4. Summary of Cell and Antibody Transfer Experiments in EAC

Group	Immunization	Cell transfer		Ab transfer
		Cells	Dose	Ab
A	—	SpC + LNC*	10^7	—
B	—	CC2 TCL*	102 to 6 × 10^6	—
C	—	CC2P12 TCL*	3.5 to 6 × 10^6	—
D	CC2P12‡	—	—	Anti-P1-P12 sera
E	CC2P12‡	—	—	Anti-CC2 sera
F	CC2P12‡	—	—	Normal sera
G	—	—	—	Anti-CC2 sera

*CC2-reactive T cells or CC2P12 with or without antibodies were administered, and the degree of inflammation and fibrosis was evaluated 3 weeks after cell transfer. The denominators in the incidence column represent the number of rats used for each experiment. SpC, spleen cells; LNC, lymph node cells; TCL, T-cell line; —, not performed.

†n.e., not examined.

‡CC2P12 was immunized, and the indicated sera (1 ml after 5-fold dilution) were injected intravenously twice a week for 5 weeks. Rats were examined histologically 6 weeks after the immunization.

§Significant differences were noted in the following comparisons: D versus F, $P = 0.03$; E versus F, $P = 0.005$.

¶Significant differences were noted in the following comparisons: D versus F, $P = 0.049$; E versus F, $P = 0.01$.

(Table continues)

epitope spreading was intensively investigated, and this immunological event was thought to be highly involved in the relapse and chronicity of autoimmune diseases.[10–12] Later, it was reported that B-cell epitope spreading is also involved in the pathogenesis of autoimmune diseases.[13,14] Notably, Bischof et al[15] have shown that immunization of mice with myelin oligodendrocyte glycoprotein, but not with myelin basic protein and proteolipid protein, induced extensive B-cell epitope spreading and chronic autoimmune encephalomyelitis. Furthermore, they observed that diversification of the B-cell reactivity did not follow a sequential cascade that is seen in T-cell epitope spreading but represented a simultaneous spread toward a broad range of antigenic epitopes. In the present study, we also observed a similar mode of B-cell epitope spreading. Many reports have suggested that autoantibodies against cardiac components play an important role in the formation of DCM.[16–20] This assumption was also supported by the finding that immunoadsorption therapy to remove IgG ameliorated myocardial inflammation[4] and improved the cardiac performance and clinical status.[21] In addition, we have also observed that intravenous immunoglobulin administration suppressed the development of CC2-induced DCM and down-regulated anti-CC2 antibody production (our unpublished observation).

It is important to analyze the nature of DCM-inducing antibodies. We induced severe EAC with extensive fibrosis by immunization with CC2P12 plus transfer of anti-P1 to -P12 antisera that had been raised by peptide mixture immunization, but could not fully reconstitute the features of EAC and DCM produced by CC2 immunization. One of the reasons for this was that in our treatment protocol, it was difficult to maintain anti-peptide antibodies at a high level (unpublished observation). Although the reconstitution experiments demonstrated that anti-CC2P1–12 antisera possessed almost the same carditis-exacerbating ability as anti-CC2 antisera, there is a possibility that antibodies recognizing the conformational epitopes with high titers elicited by CC2 immunization but not by CC2P12 immunization are involved in the processes of DCM formation. In this regard, we are currently generating monoclonal antibodies against conformational epitopes of the CC2 molecule to test their ability of producing DCM. The conformational epitope mapping analysis would be helpful to identify pathogenic antibodies.

Increasing information about the pathogenesis of DCM will provide more chance for immunotherapies for the prevention and/or cessation of DCM. If pathogenic antibodies are identified more accurately, then specific and selective immunoadsorption could be achieved effectively with minimal side effects. In cases of DCM developed in a manner similar to that shown in the present study, intravenous immunoglobulin therapy, which is already in clinical trials,[22] is expected to be effective. Another important aspect is the timing of treatment initiation. As demonstrated in the previous[5] and present studies, histological examination revealed that fibrosis of the heart starts at 4 weeks PI and establishes at 6 to 8 weeks PI. Generation of the full range of pathogenic antibodies starts at the same period of time. Therefore, this time point is critical for the start of treatment. Improvements in the image analysis and functional studies are expected to greatly increase the effect of DCM therapy.

In summary, we identified the amino acid residue containing carditis-inducing epitope(s) in the CC2 molecule. By comparing CC2-induced EAC and subsequent DCM with peptide-induced EAC, it was demonstrated that B-cell epitope spreading is critical for the development of DCM. Importantly, by down-regulating pathogenic antibodies, it is possible to control the disease processes. Information obtained in the present study will provide useful information for the development of effective immunotherapies against human DCM.

Acknowledgment

We thank Y. Kawazoe for technical assistance.